Order Number 9432341

Infrared vehicle sensor for traffic control

Hussain, Tarik Mustafa, Ph.D.

City University of New York, 1994

U·M·I

300 N. Zeeb Rd.
Ann Arbor, MI 48106

INFRARED VEHICLE SENSOR FOR TRAFFIC CONTROL

by

TARIK MUSTAFA HUSSAIN

A dissertation submitted to the Graduate Faculty in Engineering in partial fulfillment of the requirements for the degree of Doctor of Philosophy, The City University of New York.

1994

This Manuscript has been read and accepted for the graduate faculty in Engineering in satisfaction of the dissertation requirement for the degree of Doctor of Philosophy.

11/4/93
Date

Chair of Examining Committee

November 4, 1993
Date

Co-Chair of Examining Committee

11/9/93
Date

Executive Officer

Professor Samir Ahmed

Professor Tarek Saadawi

Professor Leonid Roytman

Professor Joseph Barba

Professor Kraimeche Belkacem

Supervisory Committee

The City University of New York

Abstract

INFRARED VEHICLE SENSOR FOR TRAFFIC CONTROL

By

Tarik Hussain

Advisors: Professor Samir Ahmed

Professor Tarek Saadawi

This thesis investigates the use of an infrared optical system for detecting and monitoring vehicular road traffic. A system was conceived for these purposes and successfully developed and tested in the laboratory using infrared laser sources and optical detectors in conjunction with computerized signal processing correlation techniques. Preliminary road tests with the laboratory equipment provided additional confirmation of the capabilities of the system to detect and monitor vehicular road traffic.

To arrive at the design parameters for a system with the potential for being low cost, low maintenance as well as effective for the purpose needed, a survey was made of possible infrared sources and detectors that could be used, with the most appropriate ones being selected and incorporated into system designs for the laboratory tests.

A complete system consisting of both the infrared laser source and optical detectors as well as the electronic processing

components required to analyze the optical signals received and further convert them into information on vehicular traffic movements was then designed and constructed. It was then tested, first in the laboratory, then in preliminary field tests at a site within the City College complex and at a location in Syracuse in conjunction with Traffic Control Technologies. The results of this work demonstrate the validity of the system technology developed and that it shows promise of being cost effective. They also show that, beyond simple vehicle monitoring and counting, the system has potential for more sophisticated applications including speed measurement and vehicle length classification.

ACKNOWLEDGMENTS

I would like to express my gratitude to all the members of my doctoral committee. In particular, I would like to thank my mentors, Professors Samir Ahmed and Tarek Saadawi, for their support and guidance in the development of this work. I would like to dedicate this thesis to my wife and my children, whose patience, great support and understanding during the course of this undertaken encouraged me to attain my goals. I also would like to acknowledge the support of Energy Research and Development Agency (ERDA) of the State of New York for this work.

Table of Contents

Chapter Three

Practical System Parameters

Chapter Four

System Experimentation and Evaluation

List of Table

Illustrations

CHAPTER 1

INTRODUCTION

1.1 IDENTIFICATION AND SIGNIFICANCE OF THE PROBLEM :

Traffic control deals with movements of vehicles (and pedestrians). Since the volume of these movements is usually not constant with time, often fluctuating from minute to minute, it is desirable to detect (sense) a movement by placing one or more detection devices (sensors) in the vehicle's path. The vehicle's motion or mere presence causes a detectable change in an energy pattern. The inductive loop detector (ILD), shown in figure 1, is the most widely used and is an example of the energy pattern change detector[1].

Traffic detectors may be applied either singly or in multiple installation, to measure presence, volume, occupancy, and speed. These surveillance measures can be used as a control parameter at an individual signalized intersection, or in a coordinated traffic responsive signal system, or for freeway operations.

Vehicle arrivals tend to fluctuate at an individual intersection, so efficiency depends on responsiveness to demand that arrives from minute to minute. An actuated green

interval is elastic in length and can be tailored to actual arrivals. The green interval can vary from the minimum to maximum settings on the controllers on the biases of unit extensions generated by vehicles crossing the detectors.

Vehicle detectors have been in use for fifty years. Various types of detectors have been developed over the decades. They range from pressure detectors, magnetic detectors, photocells, radar detectors, sonic detector, inductive loop detectors(ILD) and magnetometers to coaxial detectors(see [2] for more details). Several experimental vehicle detectors show impromise of improvement over the ILD type. Examples are the self-powered vehicle detector, the passive bus detector, the micro loop detector and the wide area detection system[2].

This dissertation focuses on the development of a reliable, low-cost, low-maintenance, easily installed infrared overhead detector. It is designed to operate under all highway environmental conditions, detect both presence (stopped vehicle) and passage (maximum speed detection 70 mph) of all vehicles types and determine speed and length of vehicles.

1.2 BACKGROUND :

Traffic control requires the measurement of the volume of vehicles and their movements. Traffic detectors singularly or in multiple installations are used to measure the presence, volume and speed of vehicular traffic. The surveillance data can then be used to provide guide-line for particular signal intersections, for coordinated, traffic responsive signal system, or for freeway operations.

Detection and control systems need to be responsive to traffic activities. For example, the number of vehicles arrive at intersections will fluctuate, so green signal intervals will need to vary to reflect approaching traffic needs, or other traffic issues. To meet these needs, detection systems must be capable of counting the number of vehicles passing in each direction along a road. For multi-lane roads, this detection capability is obviously desirable on an individual line basis. As traffic control technology becomes more sophisticated, particularly in urban areas, measuring vehicular speed and type (truck or passenger) as well as measuring numbers of vehicles approaching intersections or other control points is possible.

Vehicle detectors have been used for more than fifty years; the most common are inductive loops or ellipses of wire

buried in the roadway. Loop detectors are of two types : short (about 1-m in length) that produce a present-absent signal, used for individual vehicle detection, and large (80-m or more in length) that deliver a signal proportional to total vehicle density[3]. These detectors record a vehicle passing over the loop. This effect is due to the fact that most vehicles are made at least partially of ferro-magnetic materials that induce an inductive "blip" of electronic current in the buried loop as they pass over it. These detectors are relatively expensive to install, they have to be buried in the road way and paved over. They may also suffer from sever weather hazard (freezing etc.) which may deteriorate pavements and effect the loops. In addition, the inductive loop detectors have indeterminate zones of influence that make them unsuited to multiple lane use. They also lack speed and length detection capabilities that increasingly sophisticated traffic control system will need to deal with heavy traffic.

This project was initiated at the City College of New York using an approach that focused on two main areas of Electrical Engineering : the use of lasers for remote sensing, and signal processing and signal correlation work.

1.3 SCOPE :

New York's Long Island Expressway has been called the world's longest parking lot, but it may no longer have that dubious distinction[4]. Most of the world's major highways are bogged down with traffic, not only in the morning and evening rush hours, but in many other times of the day. A 1986 traffic study of 29 major U.S. cities by the TEXAS Transportation Institute, College Station, estimated that US $24 billion per year was lost in these cities alone because of congestion. In each of nation's 12 largest metropolitan areas, losses exceed $1 billion per year.

The great hope for alleviating some of all of these conditions is a concept called Intelligent Vehicle-Highway System (IVHS) in the United States, Road Transportation informatics in Europe and Japan has similar programs. The basic goal of these programs are the same : to incorporate a range of technologies and ideas to improve mobility and transportation productivity, enhance safety, maximize the use of existing transportation facilities and energy resources, and protect the environment. Therefore, the rapid progress in computers, communications, and controls has made possible practical technical solutions to many highway problems that may have been unattainable otherwise.

Some of the needed IVHS components have already been put in place on a limited basis-traffic signal controls, vehicle identification systems, automatic tool charging, and variety of driver information and navigation aids. But IVHS would use an overall systems engineering approach to implement, step by step over perhaps the next 25 to 30 years, a logical approach to the ultimate scenario of smart cars on smart highways.

In the following sections, we survey the different approaches for traffic monitoring :

1.3.1 Inductive Loop Detectors:

These are the most common methods of data acquisition for traffic monitoring and control[3]. Loop detectors are of two types: short(about 1-m in length) that produce a present-absent signal can be used for individual vehicle detection, and large (80-m or more in length) that deliver a signal proportional to total vehicle density with their range. Magnetic loops can provide enough data for calculation of average speed, vehicle flow, and vehicle density. They are, however, very inflexible since any modifications and additions require digging grooves in the road, thus producing traffic disturbances, see figure 1. In addition, they cannot be used for more sophisticated tasks such as queue length measurements, tracking, etc.

1.3.2 Image Processing Techniques:

For almost two decades, research has been conducted on the use of video images for obtaining the desired traffic data. The earliest reported research into the application of image-based systems for traffic monitoring was performed at the University of Tokyo[5]. In the early 1980s at the University of Tokyo, Institute of Industrial Science, experiments were conducted to demonstrate that traffic-flow data could be obtained in real time from TV data. In 1978, FHWA contracted the Jet Proplution Laboratory (JPL) to investigate the feasibility of using video sensors and image processing for automatic traffic monitoring and to develop a breadboard system. This represents the first significant U.S. effort to apply imaging technology for automatic traffic monitoring.

Video detection by video cameras is one of the most promising new technologies for wireless data collection and implementation of advanced traffic control and management schemes such as vehicle guidance/navigation. Autoscope is the most resent worldwide development detection system in the U.S.[6]. The Autoscope can detect traffic in many locations within the camera's field of view. These locations are specified by the user in a matter of minutes using interactive graphics and can be changed as often as described. This

flexible detection placement is achieved by placing detection lines along or across the roadway lanes on a TV monitor displaying the traffic scene. Every time a car crosses these lines, a detection signal is generated by the device. This signal is similar to that produced by loop detector. However, the advantage is that, in addition to the wireless detection, a single camera can place many loops, thus providing true wide-area detection.

1.3.3 A Two Frequency Radar Techniques :

The use of a side-looking in conjunction with a sidewall reflector is one possible mean of obtaining lateral position information for use in vehicle automatic lateral control. Conventional electromagnetic methods appear to be the most feasible. Essentially, an ultra-short-range radar operating at frequencies that are unaffected by changes in the environment is needed. The general configuration is shown in figure 2. The parameter R_0 is used to present the desired lateral position of the vehicle as measured with respect to the sidewall reflector. The actual position will be denoted by d[7].

When implemented and deployed on a controller vehicle, an ideal radar would measure the distance d. Knowing R_0, an error signal will be generated and supplied to the controller

which would act to maintain the vehicle at R_0. Perturbations in position about R_0 are to be expected due to the random external forces acting on the vehicle.

The following are few promising systems that could be utilized:

1- A continuous-wave (CW) radar.

2- An AM-CW radar.

3- A two-frequency radar.

4- A two-frequency Doppler radar.

5- An FM-CW radar.

6- A short-pulse baseband radar.

The CW radar system is the easiest to implement. It operates by transmitting single sinusoidal wave of radian frequency W. The frequency of the received signal is then measured, consequently, a phase difference is determined. Hence, the distance is obtained. However, the measured phase can only be determined within +180 & -180. Since a total round trip path of wavelength λ will introduce a total phaseshift of 360, the maximum unambiguous range d_{max} which can be determined by the radar is,

$$d_{max}=\lambda/2 \qquad \textbf{(1.3.3.1)}$$

where λ = 2 c/w, and c is the velocity of light.

Thus, a wavelength of 4m would be needed for R_0 =2 m. Unfortunately, at this wavelength, the size of the antenna is quite large. At shorter wavelength the antenna could be smaller, but the range would be ambiguous.

The AM-CW radar system overcomes this ambiguity problem. It determines the range by measuring the phase difference between the transmitted and echoed signals. However, it uses an Amplitude-modulation signal to achieve that.

The two-frequency radar system is similar to the AM-CW radar. (An AM-CW radar with suppressed carrier is a two-frequency radar). It utilizes the phase difference of the difference-frequency signal to obtain a distance measurement. This difference frequency determines the maximum unambiguous range.

The two frequency Doppler radar offers another approach to detect a vehicle and determine its speed. These radars are of monostatic type, where the transmitter and the receiver employ a common antenna or a bistatic type[8]. The Doppler frequency represents the amount of change in the reflected signal from the vehicle compared to the transmitted one and is given by:

$$f_D=2\frac{V}{\lambda} \qquad \textbf{(1.3.3.2)}$$

where λ is radar wavelength and v is the vehicle's velocity.

There are two Doppler's frequency techniques, the first one called the Oblique Monostotic Doppler Radar in which the vehicle velocity vector is constant and oriented obliquely to the radar slant range vector, see figure 3, and the Doppler frequency f_D is given by :

$$f_D = 2\frac{v}{\lambda}\cos\theta \qquad \textbf{(1.3.3.3)}$$

where θ is the angle between velocity and range vectors. The radar frequency in this technique is 10.5 GHZ. The disadvantage of this approach is that a highway of width 50 ft is assumed to handle three lanes of high speed traffic. It is noted that if a vehicle is travelling at a constant speed, the radar will incorrectly indicate continuous declaration and eventually indicate zero speed when the vehicle is abreast of the radar.

The second technique is called a bistatic Doppler radar. In this approach, the transmitter and receiver are located on opposite sides of the highway, and the vehicle is assumed to be travelling at a constant velocity v in direction perpendicular to a leakage path between the transmitter and the receiver as shown in figure 4. The bistatic Doppler

frequency is given by:

$$f_D=\frac{V}{\lambda}(\cos\theta_T+\cos\theta_R) \qquad \textbf{(1.3.3.4)}$$

where θ_T is the vehicle heading angle from the transmitter, and θ_R is the vehicle heading angle from the receiver. In this approach the vehicle speed error is reduced.

A conventional FM-CW radar can not measure very close range with the needed resolution. A modified form of the FM-CW radar was developed by Marukawa and Namekawa[9]. Their system measures short distances with an accuracy equal to approximately one-half the carrier wavelength.

Another clever scheme for measuring short distances is described by Nicolson and Ross[10]. In their paper, on short pulse baseband radar, they achieved resolutions less than 30.48 cm for a distance of 15.24 m.

1.3.4 Signal Processing Technique :

The velocity of a vehicle is conventionally measured by a tachometer mounted on the axile. Because all wheels of modern railway engines transmit motive power by friction there

always exists slip between the wheels and the rail surface. Therefore the conventional tachometer will not measure the exact translation-velocity of the vehicle relative to the ground. This leads to considerable errors when calculating the distance as the integral of the estimated velocity[11].

Another reason for measuring the exact speed is to render possible slip control in order to increase the economy of railway operation or to minimize the breaking distance.

Signal processing techniques are used in many engineering applications. One of these applications are a signal processor for a noncontact speed measurements systems. This system was developed for an industrial contract and is specially tailored to the conditions of railway application. Here the velocity is obtained by estimating the time delay between two stochastic signals that are generated by an optical sensor.

This technique is using the idea of estimating the time-delay between two signals generated by two optimal sensors located at distance L apart. Due to surfaces irregularities these signals are random, but nearly identical except for a time delay corresponding to the velocity of the vehicle. The estimate of the time delay is determined by detecting the maximum peak of the correlation function (open-loop estimator). The other possibility is the generation of an

error signal as a function of the estimation error ($D-\hat{D}$) from the differentiated correlation function and its corresponding feed back on a variable delay line (close-loop estimator)[11]. In the low-speed range the large variation of delay leads to stability problems on using a closed-loop system. While , in the high-speed range the required accuracy can only be achieved by an enormous hardware expense using an open-loop system. Therefore a combined structure , shown in figure 5, was developed which the open-loop estimator covers the velocity range < 2 m/s and the closed-loop estimator operates from V > 1 m/s to V = 80 m/s.

The system has two optical subsystem, located a distance L apart illuminate the rail surface with infrared light,see figure 6. The reflected light is converted into electrical signal by photodetectors. Each sensor signal represents an image of the passed rail-surface, so that ideally they are identical except for time delay.

The optical subsystem is mounted on the bogie close to the rail surface. Vertical distance variations due to the spring loading or the wear in the wheels only blur the sharp scanning slits and have no influence on the delay, because both system are identical.

The advantage of using an optical sensor in contrast to other solutions such as radar, is a higher mastermind accuracy and this is achieved by employing scanning slits that are narrow enough in the direction of motion to sense the fine structure of the rail surface. Therefore, the sensor signals have high frequency components, which yield a sharp peak in the cross-correlation function. The high selectivity of the sensor is of particular importance at lower velocities, since signal bandwidth is directly proportional to the velocity of the vehicle.

In the open-loop estimator, each sensor generates a stochastic signal whose amplitude in time is determined by time dependent location of the sensor. The delay gives the time that the second sensor will take to reach the present position of the first estimator. Because of the time-variable velocity the delay is time-varying too. That means that on signal is time-compressed, respectively, expanded version of the other.

In this subsystem the acceleration is a stochastic process and the delay can be viewed as approximately constant only over a sufficiently short estimation interval T_e. The estimator structure is shown in figure 7, which performs the short-time cross-correlation $R\hat{}(D-D\hat{})$ between the two signals.

$$\hat{R}(D-\hat{D}) = \int^{T_e} Y_1(t-D)\, Y_2(t-D)\, dt \qquad \textbf{(1.3.4.1)}$$

for a set of values of the trial parameter D_i. The value for which the function above is maximal gives the most likely estimate. A necessary condition is that the change in D over the estimation interval T_e is smaller than a fraction γ of the correlation time , which is inversely proportional to the bandwidth B of the signals.

$$\dot{D}.T_e < \frac{\gamma}{2B} \qquad \textbf{(1.3.4.2)}$$

with T_e estimation interval, B bandwidth of the signal, and γ constant value, typical $\gamma < 0.5$. This equation determines the observation time T_e. But the derivative of the delay D with respect to time is inversely proportional to V^2.

$$\dot{D} = \frac{L dv}{V^2 dt} \qquad \textbf{(1.3.4.3)}$$

the largest values of $\dot{D}$ are found for low velocities.

For the precise measurement of higher velocities another estimator structure, the delay locked loop (DLL), is implemented. The DLL is a feed back system that automatically

adjusts a variable delay D^ to the true delay D. This estimator computes only one point of the differentiated cross-correlation function at the location of the delay estimate D^. The expectation of this value is an odd function of the difference D^. Therefore, it can be integrated to control the variable time delay D^ in such a way, that the expected value of the integrator input equals zero. The linear range is limited to small errors of a few percent while for large errors the restoring force vanishes completely. Temporarily, the DLL can lock to a false maximum, because it calculates only one point of the correlation function and so it can not distinguish a local extremum from the true one. Therefore, any operation of the closed loop estimator requires a start-up procedure prior to the tracking period where it produces estimates of a small variance. The dynamical properties of this loop can be accommodated by a loop-filter of arbitrary order.

1.3.5 Law Enforcement Speed Measurements Systems:

1.3.5.1 Based On Doppler Principle:

Radar speed-measuring devices operate on the well-known Doppler principle, which relates the frequency shifts in reflected radiation to the relative velocity between the reflecting object and the observer[12]. Exiting radar devices transmit a continuous signal at either 10.525 GHZ in the X

band or 24.15 GHZ in the K band, and they analyze the reflected signal for frequency shifts that indicate the speed of vehicles in the path of beam. Each mile per hour of target speed produces a frequency shift of 31.4 Hz with the X-band frequency or 72.0 Hz with the K-band frequency.

The radar device mixes the incoming signal with a portion of the unshifted signal to obtain the frequency shift as a beat frequency, or a series of frequencies if a number of targets are within the beam. A processor then selects a target from among the various return signal. Typically, the processor will select either the strongest or the fastest return signal, depending on the relative strength of the two. A phase-locked loop the "locks onto" this target and feeds its frequency shift into a digital display that is calibrated in miles per hour.

1.3.5.2 Based On Sound Principle:

As a target approaches a sonic detector from a great distance; the audio signal will be heard, while the display is still blank. As the target gets closer, signal strength increases, since the pinch of the audio tone is proportional to the target's speed. Target signal strength also continues to increase and reaches a threshold at which it is sufficiently strong to be processed and display by internal

electronics. As the target approaches, the signal strength reaches a level that saturates the AGC, thereby saturating the audio tone. If the radar device is operated in the moving mode, when the police car is itself moving, an additional circuit function acts to determine and subtract out the speed of police vehicle. The device tasks the strong ground-return bounced off objects close to the highway as a measure of the Doppler shift created by the police vehicle's own motion, subtracts the resulting velocity from that of the target vehicle, and feeds the result into a digital displays as target velocity. Typically, in the moving mode, the officer is searching for violators on the opposite lane. Those in his own direction ca be just as easily detected by pacing them.

1.3.5.3 Across The Road Lasers (Vascar):

These devices are active because they transmit an optical energy[13]. Vascar relies on visual observation by law enforcement officers for its input. It operates on the time-distance principle and may operate in either the stationary or moving mode. Distances may be programmed into the device via a thumbwheel switch or measured using a transducer connected to the patrol vehicle's transmission (figure 8 shows a setup of the system). The transducer produces 10,000 pulses per mile (0.161 meter per pulse).

In monitoring traffic and clocking suspected speeders, the law enforcement officer measures the time it takes them to travel a known distance. When the motorist enters the operational area for a clocking, the Vascar operator throws a switch to start measuring the time interval. And, when the vehicle leaves the operational area, a stop switch is thrown. Vascar automatically determines the speed of the target vehicle by computing the ratio of the distance traveled to the lapsed time and displays this speed on a digital readout.

1.3.6 Toll Collection Techniques :

1.3.6.1 Electronic Toll Collection (ETC) :

The Automatic Vehicle Identification (AVI) system are the central feature of ETC. AVI techniques is used to identify vehicles as they pass certain points on the road, with out requiring any action by the driver or an observer[14]. AVI systems comprise three functional elements :

1- A vehicle mounted transponder (tag)
2- A roadside reader unit with its associated antenna
3- A computer system for processing and storage of data

AVI systems use a microwave signal techniques, therefore, these system can transmit and receive on a wide range of frequencies in the KHZ-GHZ ranges and they can transmit data at a very high rates. In addition , these systems are

electronic waves with a shorter wavelength than those of visible light.

As an example, phillips Industries have developed an identification system which takes the advantage of microwaves and is known as programmable remote Identification system (PREMID). It is two essential components are the identification tag and the communicator. It can read static tag information as well as programming additional or completely a new information into the tags. The communicator interrogates the tag by sending out a microwave signal. In PREMID, the transmitted signal is modulated and reflected back to the communicator from the tag. The same communicator may be used for programming a new information to tags and for information exchange with control system.

The tag contains a battery with a life expectancy of 5-10 years to make possible to store data in RAMs or shift registers [14]. While the communicator consists of one or more microwave antenna and one central electronics unit and operates at 4.5 GHZ.

This device can read and programmed between 0.1 and 4.5 m from the antenna. It has also, a positioning tolerance which allows a relative position of the tag plus or minus 45 degrees tilt, pitch and rotation and is capable to read the code of a

passing vehicle up to more than 60 kph.

1.4. OBJECTIVE :

The thesis objective is to demonstrate the basic feasibility and establish design parameters for an infrared overhead vehicle-counting detector that would have the potential to measure vehicular speed and length as well as the potential for multi-lane use.

The system to be developed and tested would use infrared laser sources and optical detectors mounted above roadways to monitor traffic. They would distinguish between the uninterrupted reflection of the infrared laser light from the road surface, no vehicle passing, and the interruption of such reflection by traffic, present of a vehicle, that would have different reflective characteristics. Then by using several laser beams to illuminate successive sections of roadway in conjunction with a computerized stochastic correlation scheme, the system would count vehicle passage and record speed and length for each traffic lane.

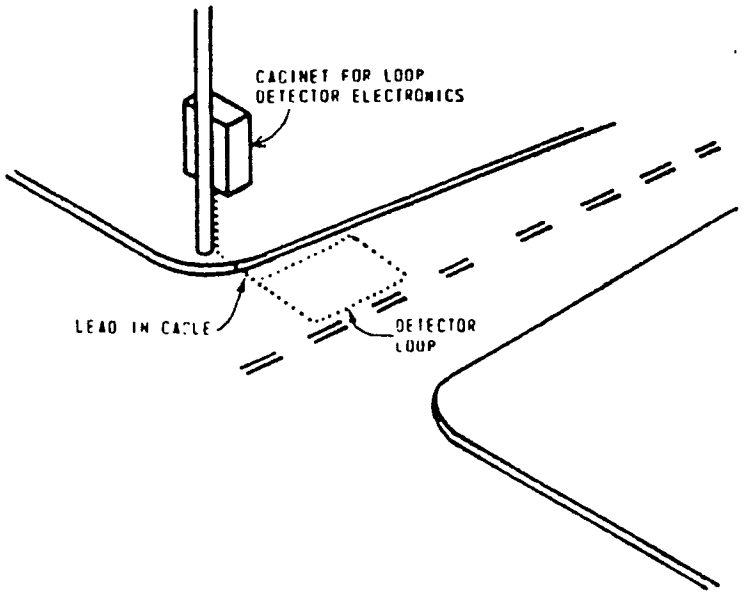

Figure.1

Typical Loop Detector Installation

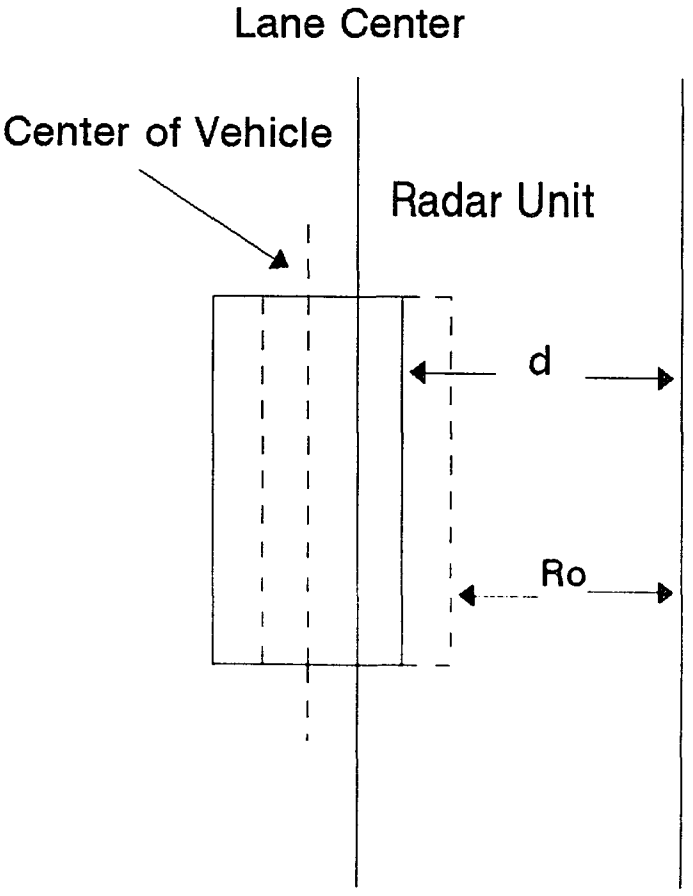

Figure.2 Vehicle Mounted Lateral position Sensor

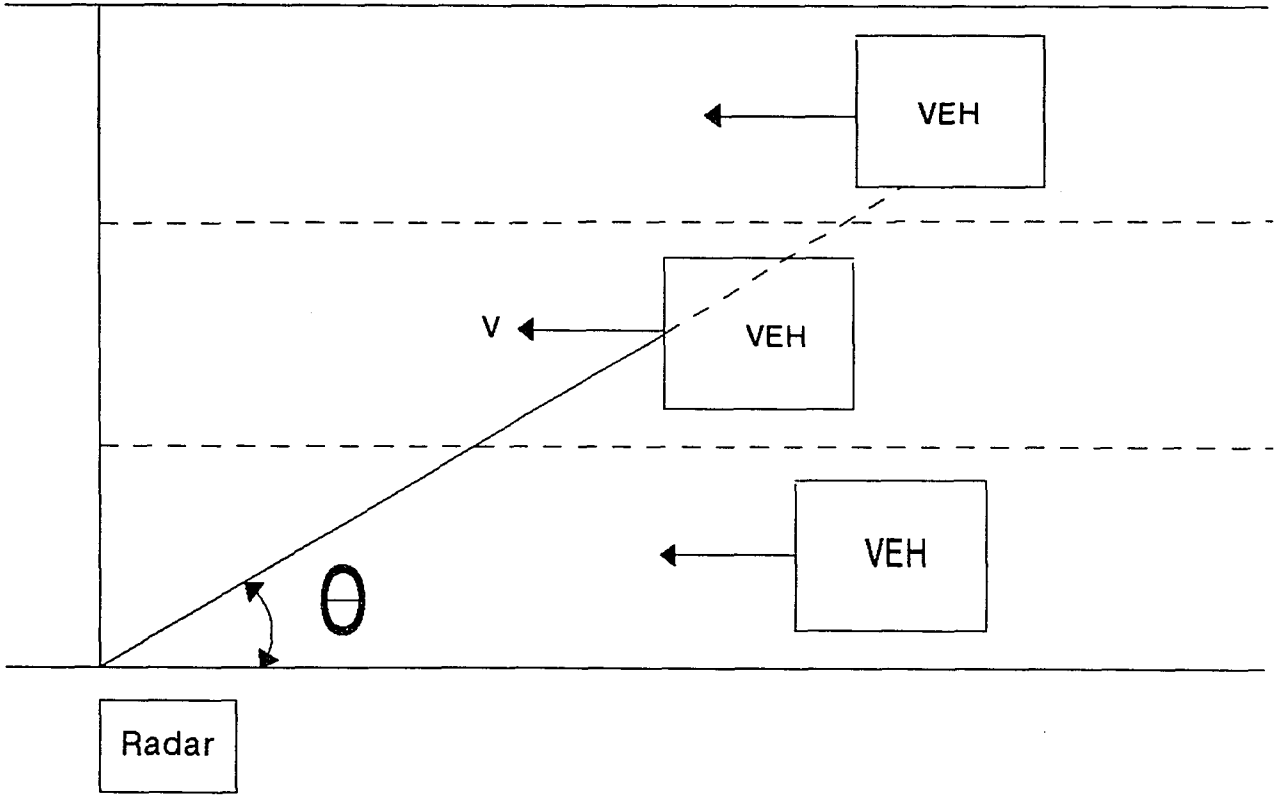

Figure.3 Oblique Monostatic Doppler Radar

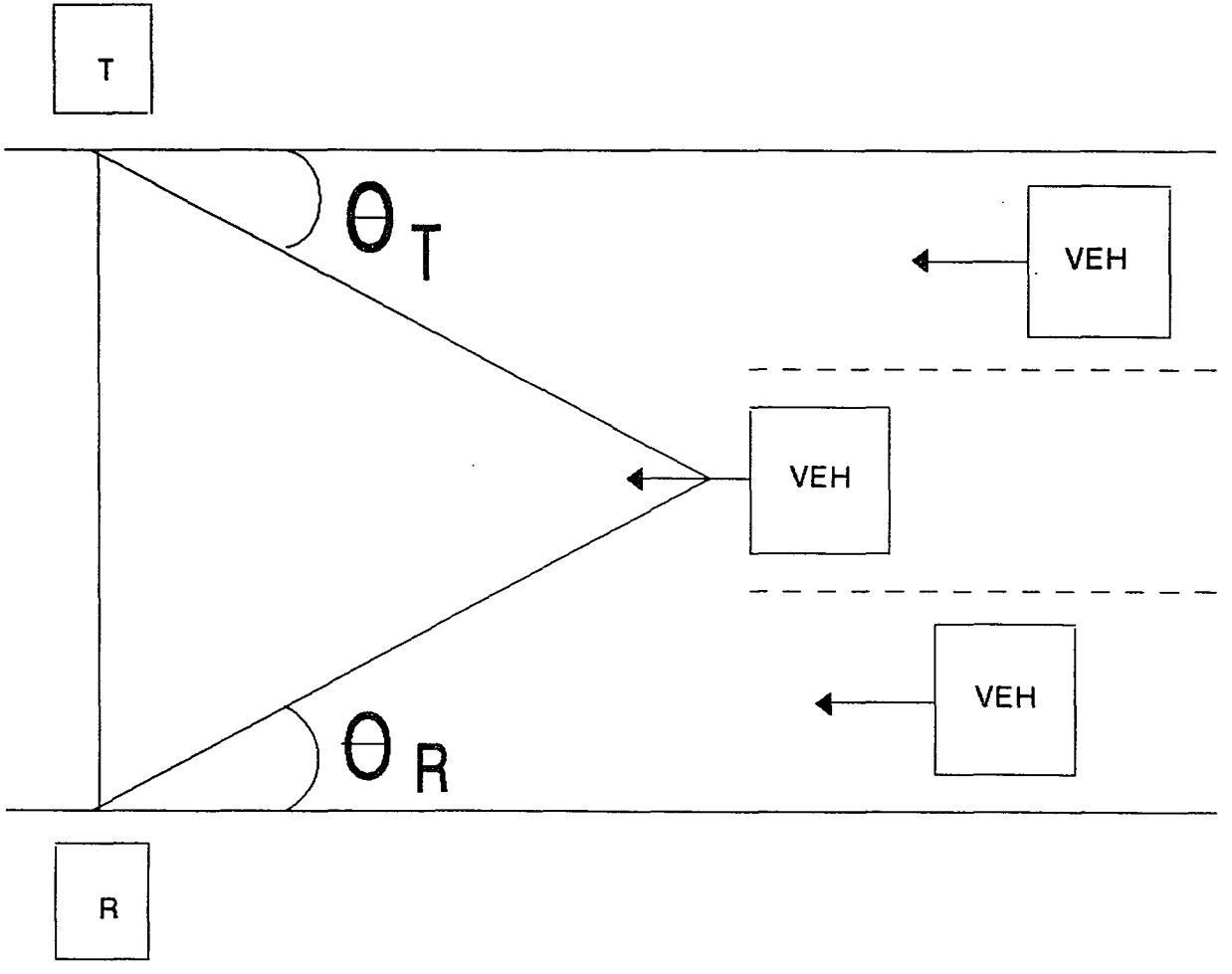

Figure 4. Bistatic Doppler Radar

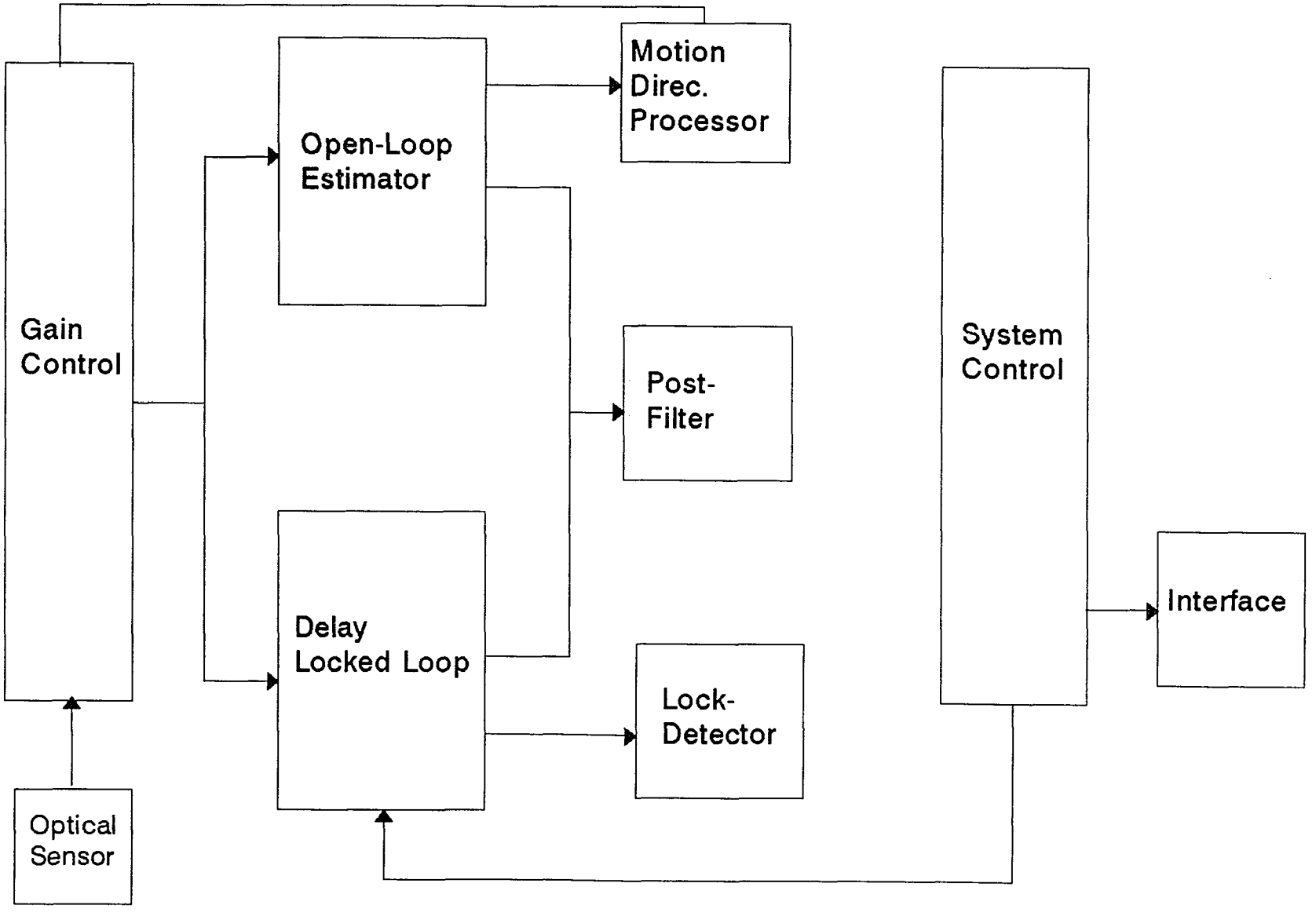

Figure.5 System Structure

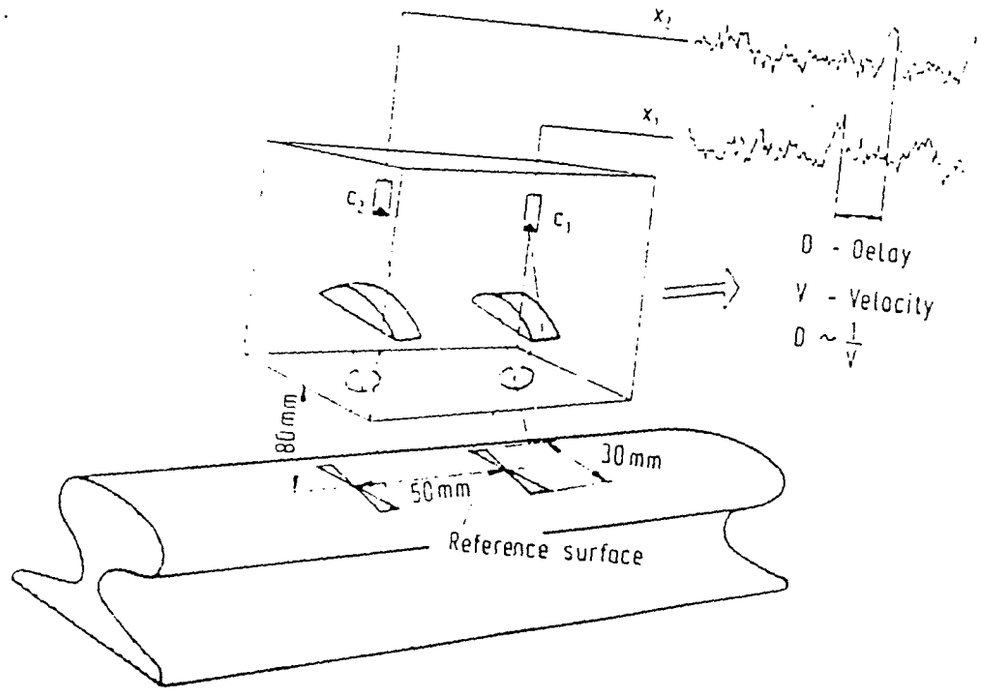

Figure.6

Principle of Optical Sensor

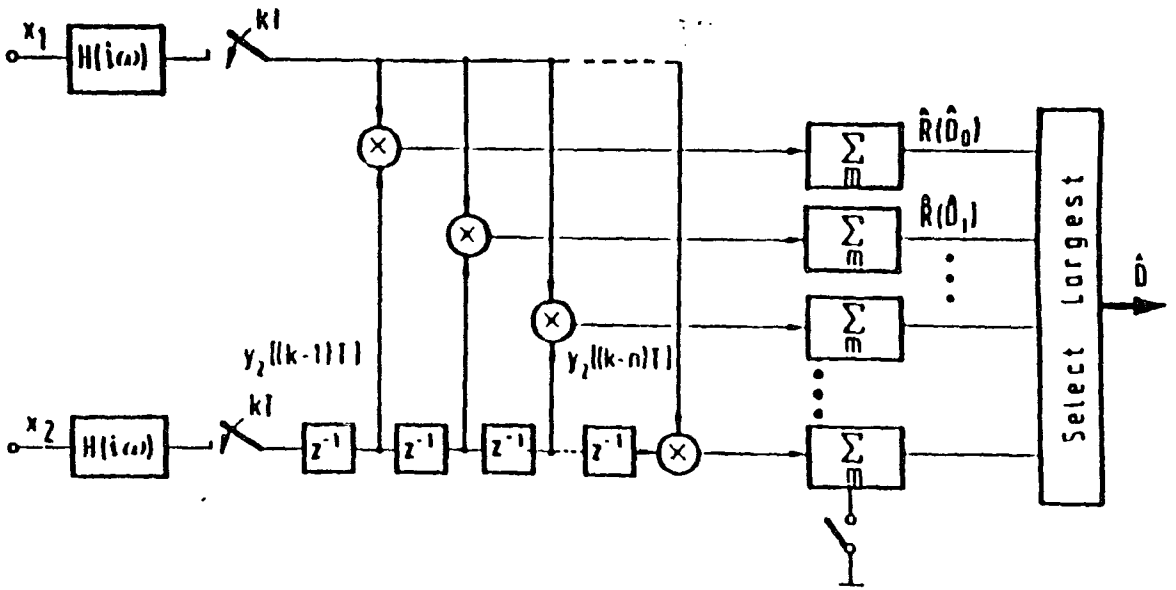

Figure.7

Structure of the Open Loop Estimator

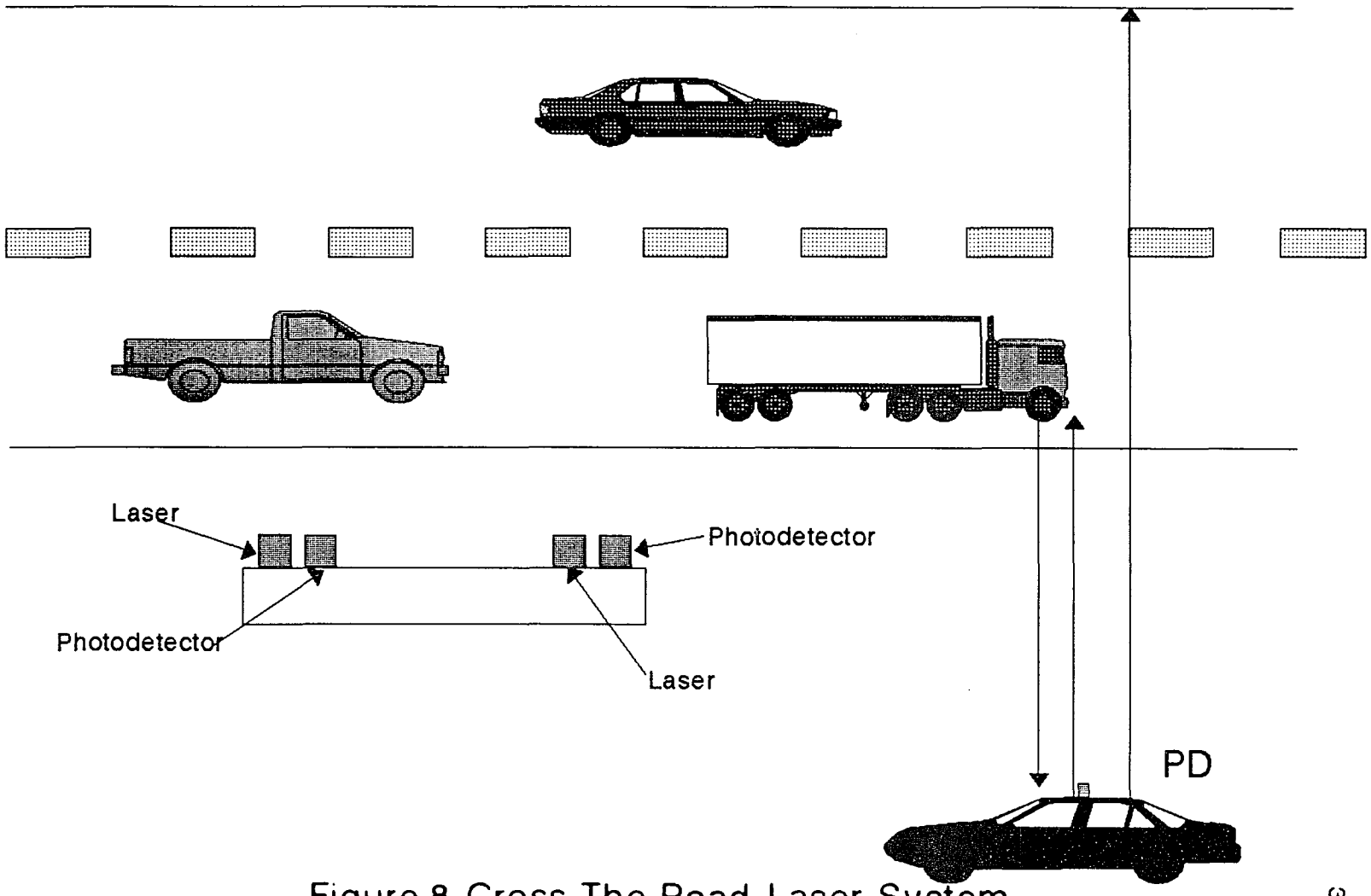

Figure 8 Cross-The-Road Laser System

CHAPTER 2

INFRARED LASER TRAFFIC MONITORING SYSTEM

2.1 System Elements :

The basic elements of the system consist of two infrared laser transceivers T1, R1 and T2, R2 (figure 9). Each transceiver is a laser source and an optical detector[15]. These are mounted on lamp standards or other elevated structures above the roadway in such a manner that they have a line of sight to the approaching traffic on the lane they are monitoring, see figure.9. The optical output of each laser beam is made narrowly elliptical in cross-section, so that at road surface it lies across an entire lane. A vehicle passing through the illuminated region makes a sharp, well defined interruption from the normal roadway surface which the laser beam would otherwise strike and be reflected from. The photodetector receivers are each aligned to view the same region of road way illuminated by the laser. The output laser beams are pulsed at a 1 kHz repetition rate. This makes for easier (i.e. higher signal to noise ratio) detection of the reflected signal by the photodetector receivers that are aligned to view the same region of roadway illuminated by the lasers.

Because of the different reflections of the infrared laser light reflected from the surface of a passing vehicle compared to the steady state reflected from the road surface, passage of a vehicle would cause significant and abrupt consecutive interruptions of the beams as it passes through theses roadway footprints, and hence cause changes in the reflected light signal picked up by the optical photodetector receivers R1 and R2. This situation can be represented , see figure 10, by the two identical transmitted optical signals Z(k) from each of the laser transmitters, T1 and T2. The reflected signals received by receivers R1 and R2 are denoted by X(k) and Y(k) respectively.

For simple vehicle counting, the interruption of any one of the beams and consequently of its reflected signal can be used to detect and count passing vehicles.

The amplitude of the reflected signals X(k) and Y(k) are affected by the presence or absence of a vehicle in the optical footprint of the laser beams directed at the road surface. Passage of a vehicle will cause an abrupt interruption or change from the steady signal that would be normally received as a result of reflections from the road surface. Furthermore, since the distance (d in figure 9) between the optical footprints of the laser beams from T1 and

T2 is fixed (since the lasers remain fixed in the direction in which they point) the delay, T_d, between the two interruptions detected by the received reflected signals X(k) and Y(k) will depend on the speed of the passing vehicle, and can in principle be used to measure it. The actual interruption duration, T_X and T_Y, in each of the received signals will depend on both the speed and length of the vehicles as they pass through each of the optical footprints. Thus if there is acceleration or deceleration between the two duration then T_X and T_Y will be different, and together with T_d can be used to determine speed, acceleration and length.

2.2 Vehicle Counting :

This is accomplished by counting the episodes where the reflected signals undergo abrupt and sustained changes from their normal road surface reflection. It is important that the circuitry and logic doing that be capable, through proper programming, of recognizing reflection signal changes characteristic of vehicles and hence distinguishing between changes due to passage of vehicles and other spurious noise changes (e.g. a bird flying across the optical beam).

There are two approaches to count the number of vehicles passing. The first approach uses the fact that the final detector envisioned must have the capability of performing

cross-correlation function in order to determine the speed and the length of the vehicle. Thus, when $R_{xz}(k)$ is greater than $R_{xzo}(k)$ (case of no interruption) indicating the passage of a vehicle, a signal increments the counter, otherwise the counter remains idle.

The second approach assumes a simple detector for counting passing vehicles only (i.e. no capability of measuring the speed or the length of the vehicle). In this case, the received signal is fed to a pre-amplifier, then to a low pass filter to produce the D.C. component. The D.C. component have two values; HIGH indicating no vehicle passing and LOW indicating the passage of a vehicle. The output of the low pass filter is fed to a comparator and then to the counter, see Figure 11.

2.3 Speed and Length Measurements :

2.3.1 Speed Measurements :

As discussed in Section 5.1 above, the speed of any vehicle, V, can be determined by dividing the roadway distance between the laser footprints of the two signals by the time delay, T_d, taken by the vehicle to cross the distance, see (figure 9 and figure 10). The speed of the vehicle is then given by:

$$V = d/T_d \qquad \textbf{(2.3.1.1)}$$

$T_d = (T_{Y0} - T_{X0})$, where T_{X0} and T_{Y0} represent the starting times of the interruptions by the passage of a vehicle of the reflected signals from the roadway to the first and second receivers respectively, (see figure 10).

To determine the time delay, T_d, between the interruptions in each of the reflected signals (X(k) and Y(k)), across-correlation technique can be used, in which the cross-correlation between the outgoing or reference and reflected signals is examined. Cross correlation for the two signals, (X(k) and Z(k)), is given by:

$$R_{xz}(i) = \sum_{K=0}^{T_e} Z(k)\,X(k+i) \qquad \textbf{(2.3.3.2)}$$

Where T_e represents the window size in pulses in which the correlation has been performed. At this stage, T_x and $T_{\cdot\cdot}$, are determined, (See figure.10).

Cross-correlation for the two signals, (Y(k) and Z(k)), is given by:

$$R_{YZ}(i) = \sum_{K=0}^{T_e} Z(k)\,Y(k+i) \qquad \textbf{(2.3.3.3)}$$

and T_e as defined above. Using equation (2.3.3.3) T_Y and T_{Y0} can be determined. Therefore the time delay, T_d, can be calculated by:

$$T_d = T_Y - T_X = T_{Y0} - T_{X0} \qquad \textbf{(2.3.3.4)}$$

The cross-correlation may be determined electronically by first digitizing, then combining the relevant outgoing and reflected signals into a digital signal-processing integrated circuit chip. The magnitude of the output signal from the chip would then be proportional to the extent that correlation exists between the reference and reflected signals.

The use of a correlation function is basically a process of shifting X(k), or Y(k), train of pulses by one pulse, multiplying with the corresponding Z(k) pulses and summing the results. The process repeats for the duration of the window. Figure 12 gives a typical sequence of operation.

In the steady state and if there is no vehicle passing , the cross correlation $R_{xz}(k)$ should be equal to a value $R_{xzo}(k)$,(see figure 12). When a vehicle interrupts the beam, $R_{xz}(k)$ would increase while reaches the maximum value when the vehicle is completely under the beam and then decrease as the car leaves the beam footprint. From these cross-correlation values (between the transmitted signals, Z(k) and reflected signals, X(k) and Y(k)), the start of the interruptions, T_{X0}

and T_{Y0}, and the duration of the interruptions, T_X and T_Y, can be determined for each of the reflected beams. Thus, Speed can now be determined by:

$$V=\frac{d}{T_d}=\frac{d}{T_{Y0}-T_{X0}} \qquad \textbf{(2.3.3.5)}$$

2.3.2 Length Measurements :

Determination of the vehicle length can be accomplished by obtaining T_x, (in figure 10), which represents the time required for the vehicle to pass the first beam, and combining that with the speed information obtained above, thus:

$$L_{vehicle}=V.T_x \qquad \textbf{(2.3.2.1)}$$

Using correlation techniques can also provide an alternative approach for counting vehicles to the technique described in Section 6.2 above. Again this would be done by counting the number of interruptions in either beam as an evidenced by the abrupt and sufficiently sustained change in the auto-correlation function.

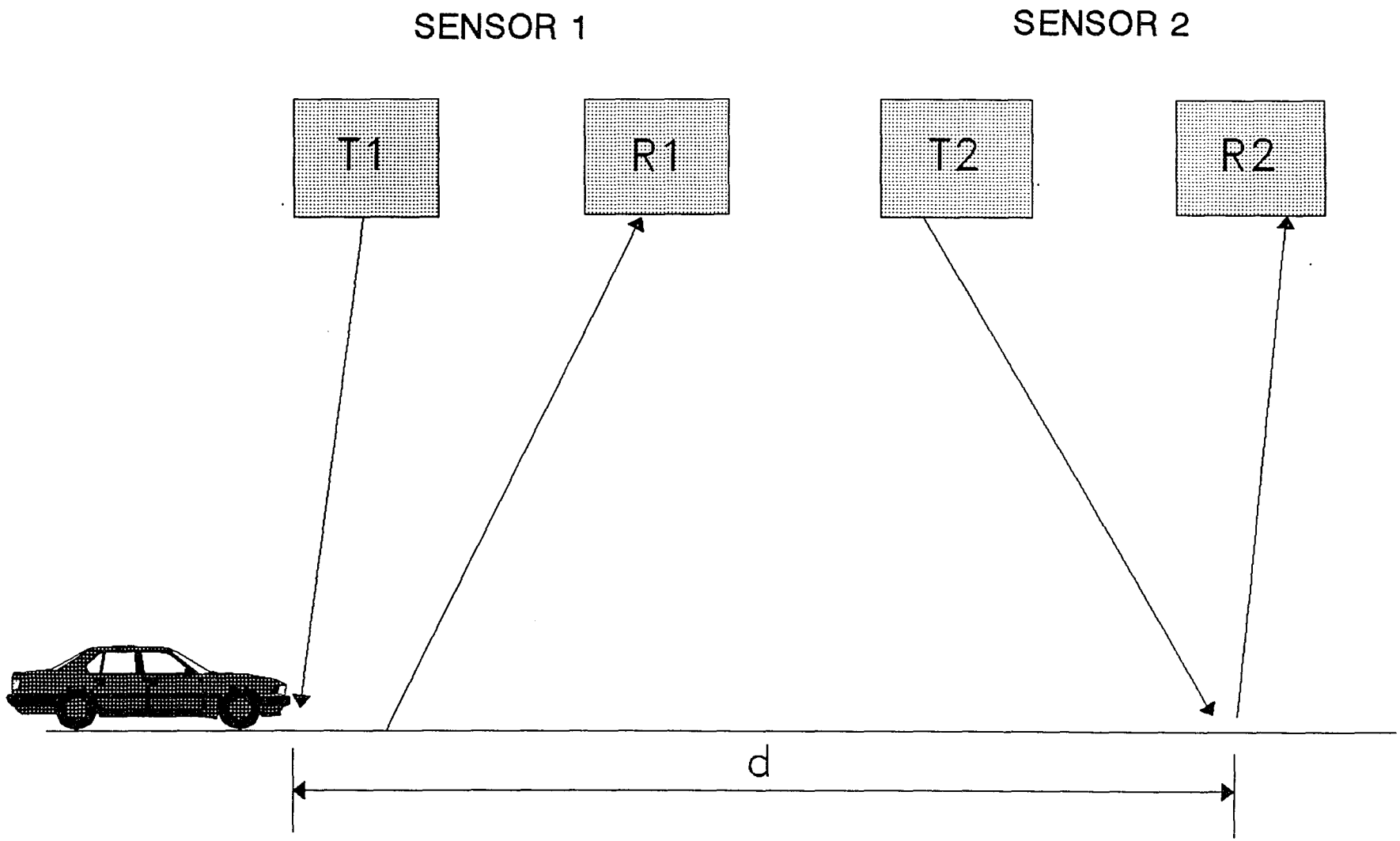

Figure.9 Signal Interruption

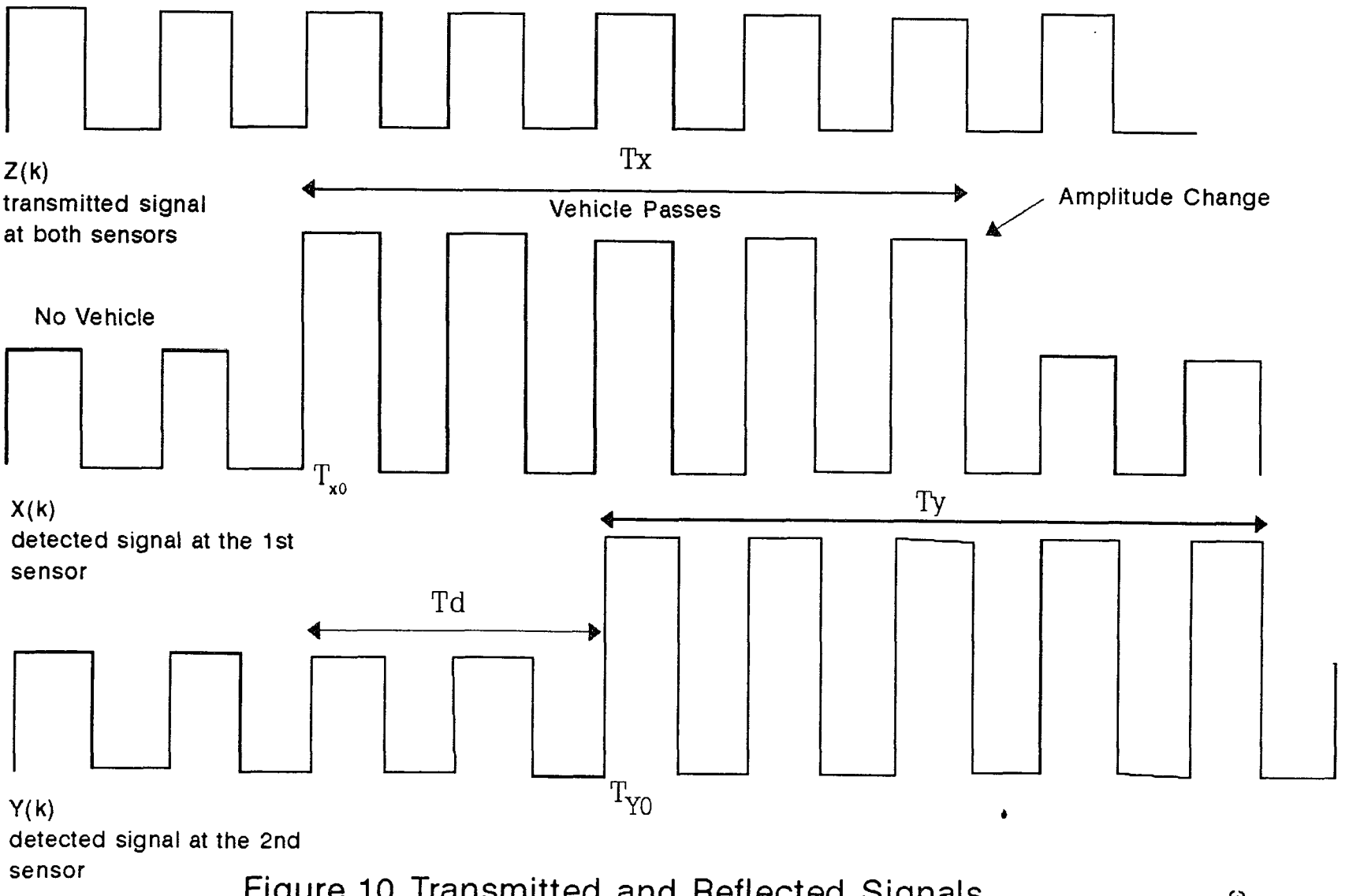

Figure.10 Transmitted and Reflected Signals

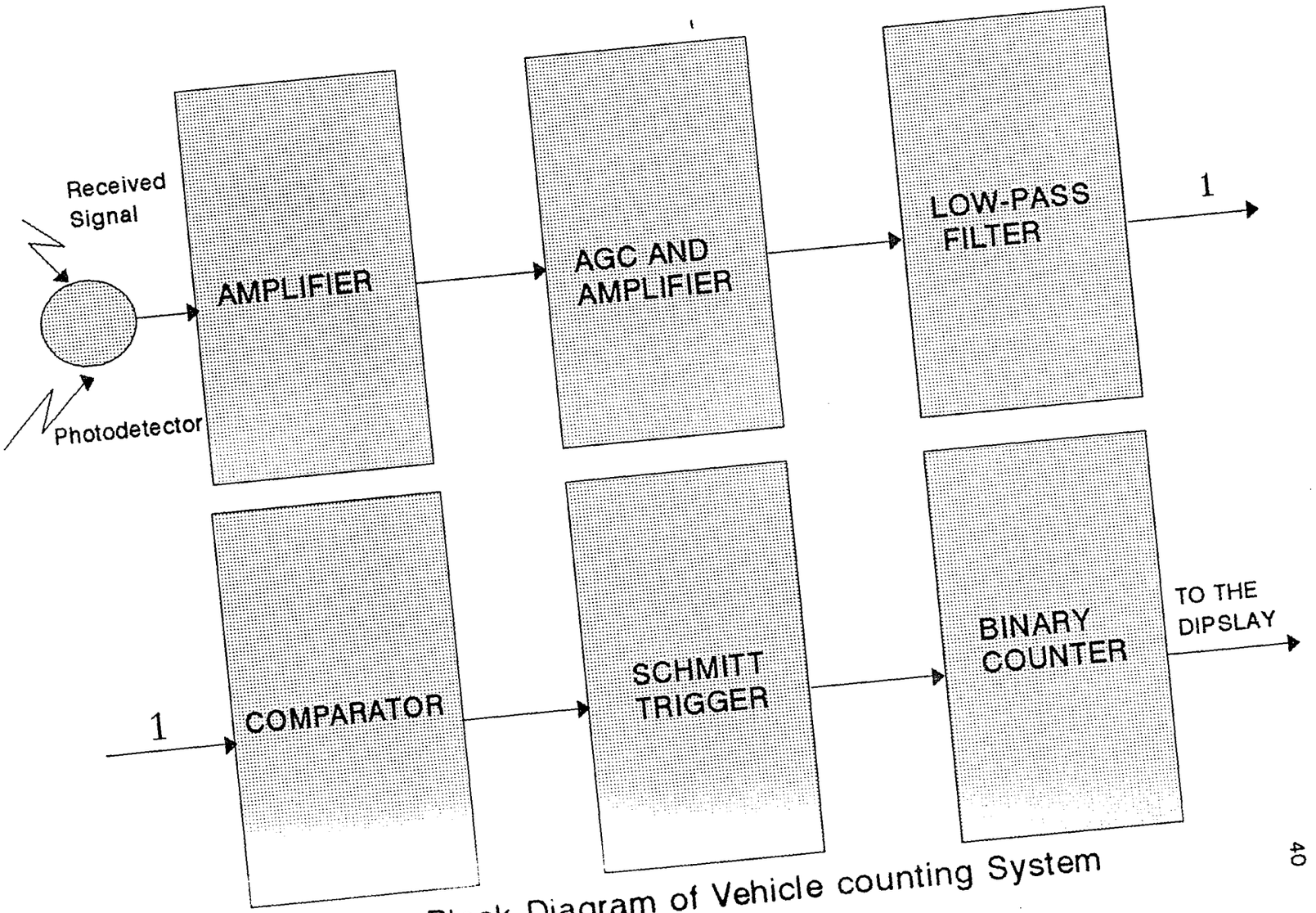

Figure.11 Block Diagram of Vehicle counting System

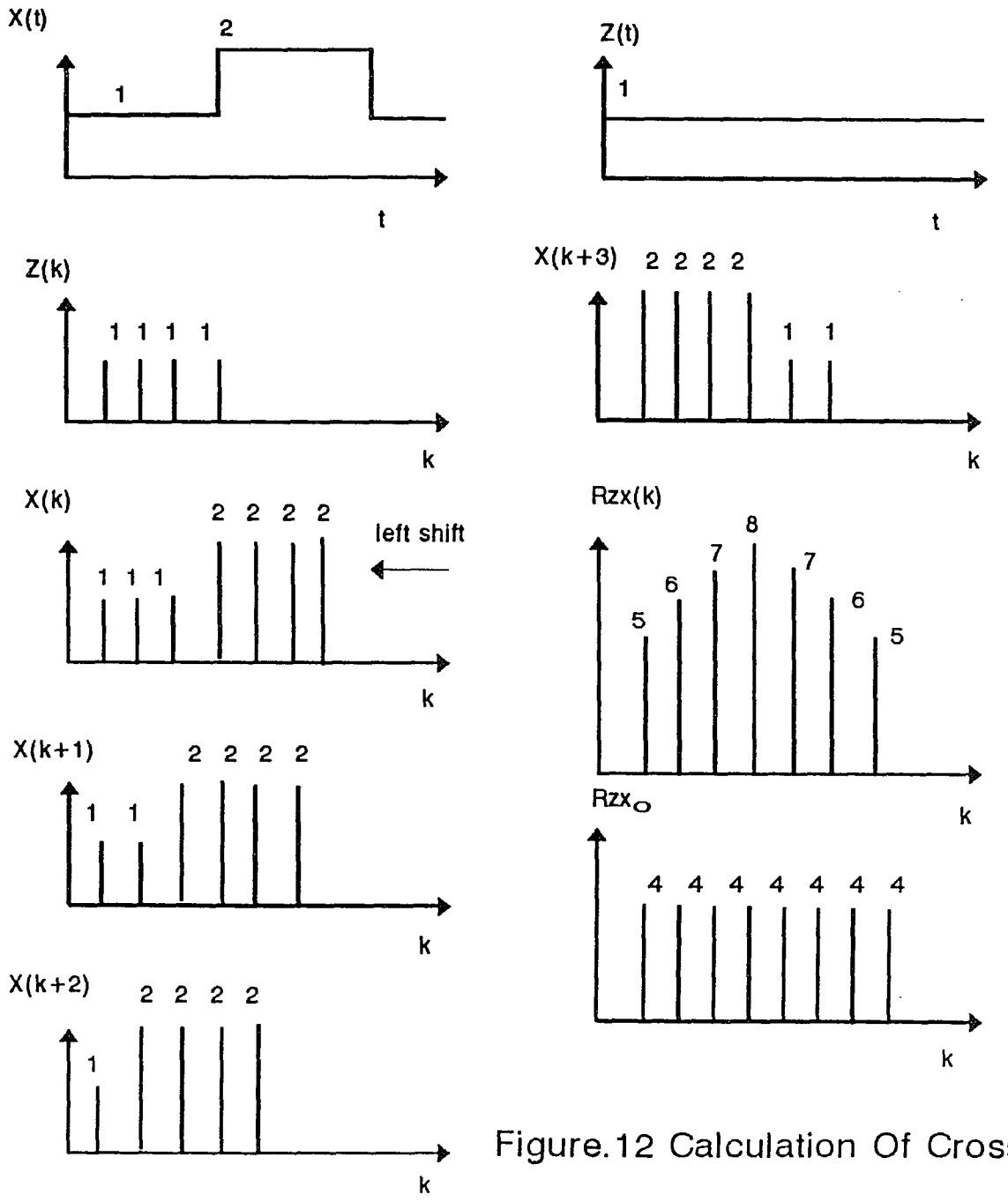

Figure.12 Calculation Of Cross-Correlation

CHAPTER 3

PRACTICAL SYSTEM PARAMETERS

3.1 The Optical Laser Transmitter And Receiver System :

To meet the practical demands expected of the system, an infrared optical transmitter and receiver system are designed to be low cost and low maintenance and easy to install[16]. Approximate cost estimates call for installed costs of approximately $500 per transceiver set (assuming quantity production). This may be compared to installed loop costs of $1800-$3200 plus disruption of traffic during loop installation.

To be reliable, the system needs to have sufficient laser output and receiver sensitivity to give satisfactory signal-to-noise ratios. To optimize signal-to-noise ratios, an infrared transceiver system operating in a pulsed mode at an approximately 1 khz repetition rate was designed. This permits tuned detectors to be used to reduce noise. The repetition rate is set high enough so that pulse intervals are short compared to the duration of changes in reflected signal caused by the passage of vehicles. In this manner, signals representing vehicle passage can be readily identified and differentiated from spurious signals.

The experimental system designed and built is shown in figure 13. A single solid state gallium arsenide injection laser diode with a pulsed output at 905 nanometers is used in conjunction with a collimator and a beam splitter to provide the two transmitted signals. Two photodiodes (with 10 nanoseconds response time) are aligned to detect reflected signals from the road surface as well as reflected signals from passing vehicles. The photodiodes outputs go into an automatic gain control amplifier(AGC) and then to a counter and displayers to count the passing vehicles (sec 6.2). The amplifier output is then fed to subsequent signal processing steps. Part of the outgoing signal is coupled, to serve as a reference for comparison purposes, into an analog-to-digital (A/D) converter and then to the signal-processing system to provide inputs for cross correlation evaluations and hence speed and length calculations.

The main components in the signal processing system are the analog-to-digital converter, the signal-processor chip TMS320C1X (TMS, to provide inputs for speed and length measurements), and the workstation I/O card model PIO-12 parallel digital I/O interface.

The analog-to-digital converter (A/D), is a PM-0820 chip with 8-bit resolution with digital outputs designed for ease

of use in microprocessor-based systems. This CMOS device offers 1.3 microseconds conversion time. It is ideally suited to a variety of A/D applications with high speed, low power and ease of use. No external sample and hold amplifier is needed in conjunction with input signals[17].

The digital-signal processor is a TMS320 16/32-bit single-chip. This combines the flexibility of a high-speed controller with the numerical capability of an array processor, offering an inexpensive alternative to multichip bit-slice processors. The high parallel architecture and efficient instruction set provide the necessary speed and flexibility to produce a MOS microprocessor family capable of executing 6.4 MIPS[18].

MetraByte's parallel digital I/O card provides a flexible interface between the data gathering and computational functions [19].

3.2 Infrared Laser Diode Sources and Photodiode Detectors:

3.2.1 Laser Diode Sources

A laser diode is a three layer device consisting of a pn-junction of n-type silicon, and p-type of gallium arsenide and a third p-layer of doped gallium arsenide with aluminum[20].

The n-type material contains electrons that readily migrate across the pn-junction and fill the holes of the p-type material, conversely holes in p-type migrate to the n-type and join with electrons. This migration causes a potential hill or barrier consisting of negative charges in the p-type material and positive charges in the n-type material that eventually ceases growing when a charge equilibrium exists. In order for a current to flow in this device, it must be supplied at a voltage to over come this potential barrier. This is the forward voltage drop across a common diode. If this voltage polarity is reversed, the potential barrier is simply increased assuring no current flow. This is the reversed bias condition of a common diode.

A diode with no external voltage applied to it contains electrons that move and wander through the lattice structure at a low, lazy average velocity as a function of temperature. When an external current at a voltage exceeding barrier potential is applied, these lazy electrons now increase their velocity to where some by colliding acquire a discrete amount of energy and become unstable eventually emitting this acquired energy in the form of a photon upon returning to a lower energy state. These photons of energy are random both in time and direction, hence any radiation produced is incoherent such as that of a light emitting diode.

The requirements for coherent radiation be in the form lockstep phase and in a definite direction. The above demands two essential requirements:

1- Sufficient electrons at the necessary excited energy levels.

2- An optical resonant cavity capable of trapping these energized electrons for simulating more and directing them.

The survey resulted in several laser diodes being selected for testing in the system. The SSL3-solid laser of single diode gallium arsenide lasers has proved to be the most effective to date, with an output peaked in the 900 nanometer range. It has output and efficiency advantages over Hamamatsu L2376 , L2376-01 and RCA SG2000 series diodes with which might also be considered for use. This diode is intended for a wide variety of applications including alarm systems and intrusion indicators. It emits in the near infrared region of the spectrum at 907 nanometers. It provides 1 kHz pulsed outputs of up to 50 watts peak power, with forward drive currents of approximately 40 amps peak and it has a very short rising and falling time (in the range of nanoseconds). The construction of these devices is such that the emitted radiant flux is essentially confined to the junction region thus assuring both low threshold current and high efficiency.

The SSL3-laser system has the following important circuits :

3.2.1.1 Power Supply :

Ac power supply is obtained via polarized plug (CO1) through fuse safety resistor (R1) and (R2), see figure 14. These are low ohm, low watt film resistor that will quickly open up in case of a gross circuit fault. Proper polarization in respect to the AC lines is a necessity to prevent unnecessary shock hazard and use of grounded test and measuring equipment. (S1) is a key switch type where the key can only be removed in the "off" position.

Diode (D1) and (D2) along with capacitors (C1) and (C2) comprise a voltage doubler eliminating the usual iron and copper transformer. The voltage across C1 and C2 is 1.4 x 230 or approximately 340 volts. Zener diodes (Z1) through (Z5) are selected to provide the proper required current pulse for the laser diode in operation. Each one of these diodes provides a 15 volt drop.

3.2.1.2 Trigger Circuit :

This circuit determines the pulse rep. rate of the laser and uses a junction (Q2) whose pulse rate is determined by

resistor (R7) and Capacitor (C4). You will notice that the maximum permissible pulse rate is determined by the laser diode rating, the RC time constant of the charging circuit and the current capability of the power supply. R7 is controllable and resistor R sets the upper pulse rate limit.

3.2.1.3 Discharge circuit :

The discharge circuit generates the current pulse in the laser and consequently is the most important section of the puller. The basic configuration of the pulse power supply is shown in figure.14. The current pulse is generated by the charging storage capacitor (C5) through SCR and laser diode (D5). The rise time of the current pulse is usually determine by Q3 while the fall time is determined by the capacitor value and the total resistance in the discharge circuit. Figure 15 shows typical anode voltage and current wave forms of the SCR during the current pulse through the diode laser.

The peak current, pulse widths and voltage of the capacitor discharge circuit are interrelated for various load and capacitance values. The peak laser current and charged capacitor voltage relationships are shown in figure 16 for several different capacitor values and typical laser types. the voltage and current limits of the SCR are also shown.

Short pulse widths provides less time for the SCR to turn on than longer pulse widths; Therefore, the SCR impedance is higher and more voltage is required to generate the same current. Figure 17 shows the current pulse wave forms for the three different values of the capacitance. The capacitor is charged to the same voltage in all three cases, i.e., approximately 200 volts.

3.2.1.4 SCR Switch :

In conventional operation of an SCR, the anode current, initiated by a gate pulse, rises to its maximum value in about 1 microsecond. During this time the anode-to-cathode impedance drops from open circuit to a fraction of an ohm. In injection laser puller, however, the duration of the anode-to-cathode pulse is much less than the time required for the SCR to turn on completely. Therefore, the anode-to-cathode impedance is at level 1 to 1 ohms through out most of the conduction period.

3.2.1.5 Current Monitor :

The current monitor in the discharge circuit provides a means of observing the laser current waveform with a oscilloscope. A resistive type monitor (R11), reduces circuit ringing and current undershoot, but the lead inductance of the

resistor may cause a higher than actual current reading. A current transformer can also be used to monitor the current and is not affected by lead inductance. Because the transformer does not respond to low frequency signals, it should be used with fast time, short pulse width and fast fall-time.

3.2.1.6 Charging Circuits :

The second major section of the puller is the charging circuit. The circuit charges the capacitor to the supply voltage during the time interval between laser current pulses, and isolates the supply voltage from the discharge circuit during the laser current pulse, thereby laser the SCR to recover to the blocking rate.

The simplest charging circuit is a resistor/capacitor combination. The resistor must limit the current to a value less than the SCR holding current, but should be as low as practical because this resistance also determines the charging time of the capacitor C5.

3.3 Photodiode Detectors

Photodiodes make use of the photovoltaic effect-the generation of a voltage across a p-n junction of a

semiconductor when the junction is exposed to light. While the term photodiode can be broadly defined to include even solar batteries, it usually refers to sensors intended to detect the intensity of light. Photodiodes can be classified by function and construction as follows[21]:

1- PN photodiodes

2- PIN photodiodes

3- Schottky type

4- Avalanche photodiodes

All of these types provide the following features and are widely used for the detection of the existence, intensity, position and color of light :

* Excellent linearity
* Low noise
* Wide spectral response
* Mechanical ruggedness
* Compact and light weight
* Long life

Photodiodes can be classified by manufacturing method and construction into five types of silicon photodiodes and two types each of GaAsP photodiodes, see table.1 .

3.3.1 Theory of Operation :

Figure(18-a) shows a cross section of a photodiode. The p-layer material at the light sensitive surface and the N-material at the substrate from a P-N junction which operates as a photoelectric converter. The usual P-type for a silicon photodiode is formed by selective diffusion of boron to a thickness of approximately 1 μm and the neutral region at the junction between the P and N layers is known as the depletion layer. By varying and controlling the thickness of the outer P-layer substrate N-layer and bottom N^+ layer as well as the doping concentration, the spectral response and frequency response can be controlled.

When light is allowed to strike a photodiode, the electrons with in the crystal structure become stimulated. If the light energy is greater than the band gap energy Eg, the electrons are pulled into the conduction band , leaving holes in their place in the valence band (see figure 18-b). These electron-hole pairs occur through out the P-layer, depletion layer and N-layer materials, and in the depletion layer the electric field accelerates the electrons toward the N-layer and the holes toward the P-type. Of the electron-hole pairs that are generated in the N-layer , the electrons, along with electrons that have arrived from the p-layer , are left in the N-layer conduction band , while the holes diffuse through the

N-layer up to the P-N junction while being accelerated, and collect in the P-layer valance band. In this manner, electron-hole pairs which are generated in proportion to the amount of incident light are collected in the N-layer and P-layer. This results in a positive charge in the P-layer and a negative charge in the N-layer. If an external circuits is connected between the P and N layers, electrons will follow away from the N-layer and holes from the P-layers toward the opposite electrode, respectively.

Different types and makes of photodetector detectors were surveyed. Several were selected for testing, including several Hamamatsu units, electroptics ET2000 and TOI units. The most promising to date turned out to be a Hamamatsu model S1337-10B4. This is a silicon photodiode. Photodiode make use of the photovoltaic effect in which a voltage is generated across a semiconductor p-n junction when it is exposed to light, see table.2. In our arrangement, the pulsed output from the Photodiode (which corresponds to the reflected light that was received from the surface of the road or passing vehicle which intercepts the outgoing laser beams) is fed into a tuned amplifier from which it goes into an analog to digital converter for further processing of the signal.

3.4 The Signal Processing and Electronic System :

The main components in the signal processing and electronic system are the analog to digital converter, the signal processor chip TMS320C1X (for speed and length measurements), and the workstation I/O card model PIO-12 parallel digital I/O interface. Below, we give a brief description of these components:

3.4.1 Analog To Digital Convertors :

The PM-0820 is an 8-bit resolution analog to digital converter, with digital outputs designed for ease of use in microprocessor-based system. A half-flash conversion technique is used, with the input signal tracked and held by on-chip circuits. No external sample-and-hold amplifier is needed for inputs signals moving at less than 100mv/μs. This CMOS device offers 1.3μs conversion time and use only 45mw of power. It is ideally suited to a variety of A/D applications where high speed, low power, ease of use, and economy of space are required[17].

PM-0820 has the following features:

1- Built-in track-and-hold function.

2- No missing codes.

3- Internal clock.

4- Single +5V supply.

5- Easily interfaced to microprocessors, or stand alone.

6- Latched 3-state outputs.

7- No adjustment required.

8- Conversion speed is 1.3μs.

3.4.2 TMS320C1X Digital Signal Processor :

The TMS320 family is 16/32-bit single-chip digital signal processor combines the flexibility of a high-speed controller with thee numerical capability of an array processor, thereby offering an inexpensive alternative to multichip bit-slice processors. The high parallel architecture and efficient instruction set provide speed and flexibility to produce a MOS microprocessor family capable of executing 6.4 MIPS. The TMS320 family optimizes speed by implementing functions in hardware that other processors implement through microcode or software. This hardware-intensive approach provides the design engineer with processing power previously unavailable on a single chip[18].

The TMS320C10 microprocessor, which is the first processor of this family, executes at 20MHZ or 5MIPS. It is capable of executing 16*16-bit multiply with a 32-bit result in a single instruction cycle. On-chip data RAM of 144 words and on-chip program ROM of 1.5k words are available.

Full-speed execution of 4K words of off-chip program memory is also possible.

TMS320 first generation has the following features:

1- 160ns instruction cycle.
2- 144/256-word on-chip data RAM.
3- 1.5/4K word on-chip program ROM.
4- EPROM code protection for copyright security.
5- 4K word total external memory at full speed.
6- 32 bit ALU/Accumulator.
7- 0 to 16 bit parallel shiftier.
8- Eight input and eight bit output.
9- Single 5V supply.
10- Packaging: 40-pin DIP.

3.4.3 Model PIO-12, (24) Bit Parallel Digital I/O Interface:

MetraByte's parallel digital I/O card provides 24 TTL/DTL compatible digital I/O lines, Interrupt and enable lines and external connections to the IBM P.C.'s bus power supplies (+5, +12, -12, -5), see figure 19. It is flexible interface for parallel I/O devices such as instruments and displays and user constructed systems and equipment[19].

24 digital I/O lines, are provided through an 8255-5 programmable peripheral interface (P.P.I.) I.C. and consist of

three ports, an 8 bits PA port, an 8 bits PB port, and an 8 bits PC port. The pc port may also be used as two half ports of 4 bits, PC upper (PC4-7) and PC lower (PCO-3), see figure 17. Each of the ports and half ports may be configured as an input or an output by software control according to the contents of a write only control registry in the P.P.I. The PA, PB, and pc ports may be read as well as written to. In addition, certain other configurations are possible for unidirectional and bi-directional strobed I/O where the pc port are used for control of data transfer and interrupt generation etc.

Interrupt handling is via a tristate driver with separate enable (interrupt enable-active low). This may be connected to any of the interrupt levels 2-7 available on the IBM P.C. and this is set by BIOS on system initialization to respond to positive (low- high) edge triggered inputs. Users must program the 8259 to respond to their requirements and set up corresponding interrupt handlers.

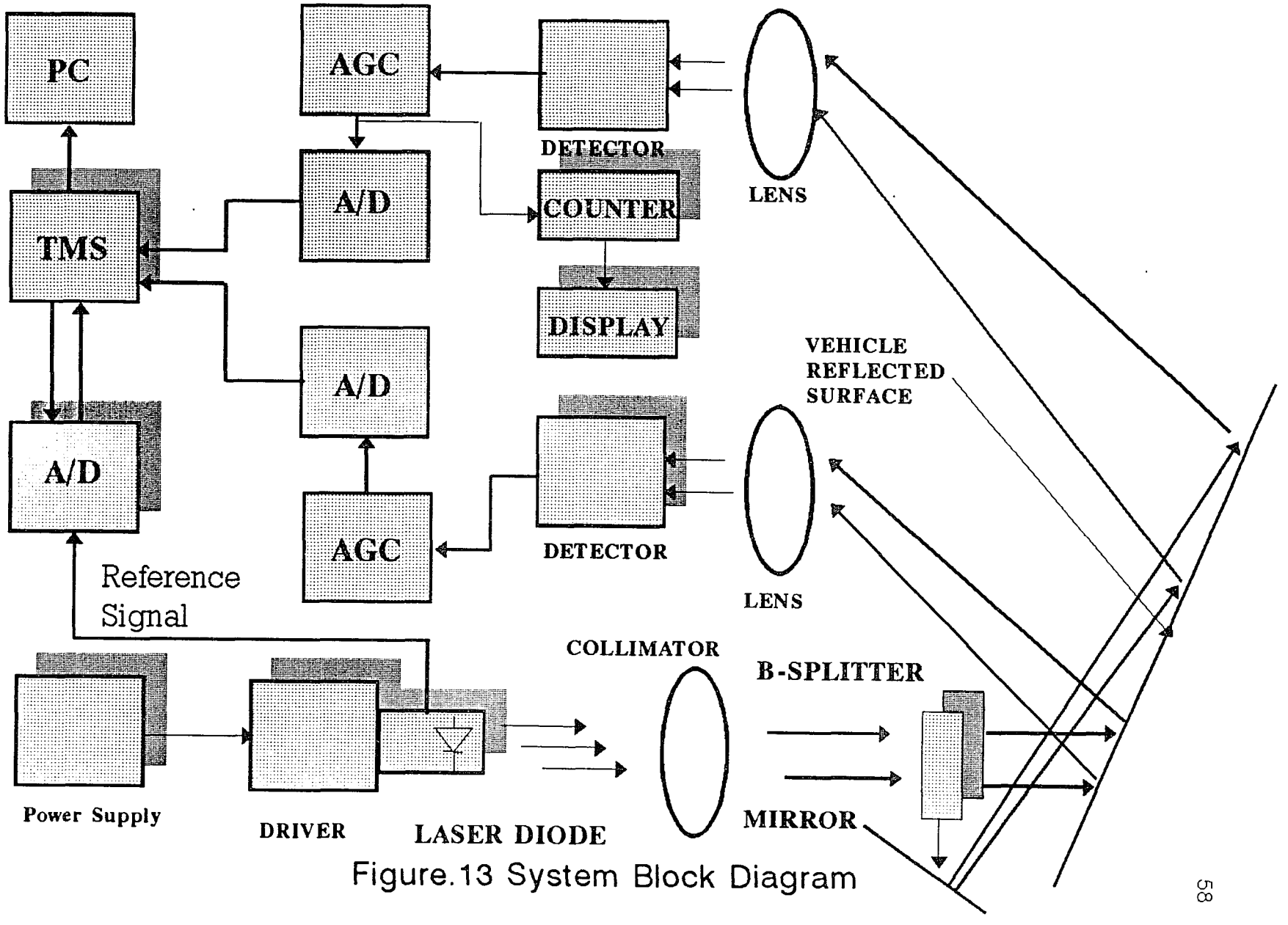

Figure.13 System Block Diagram

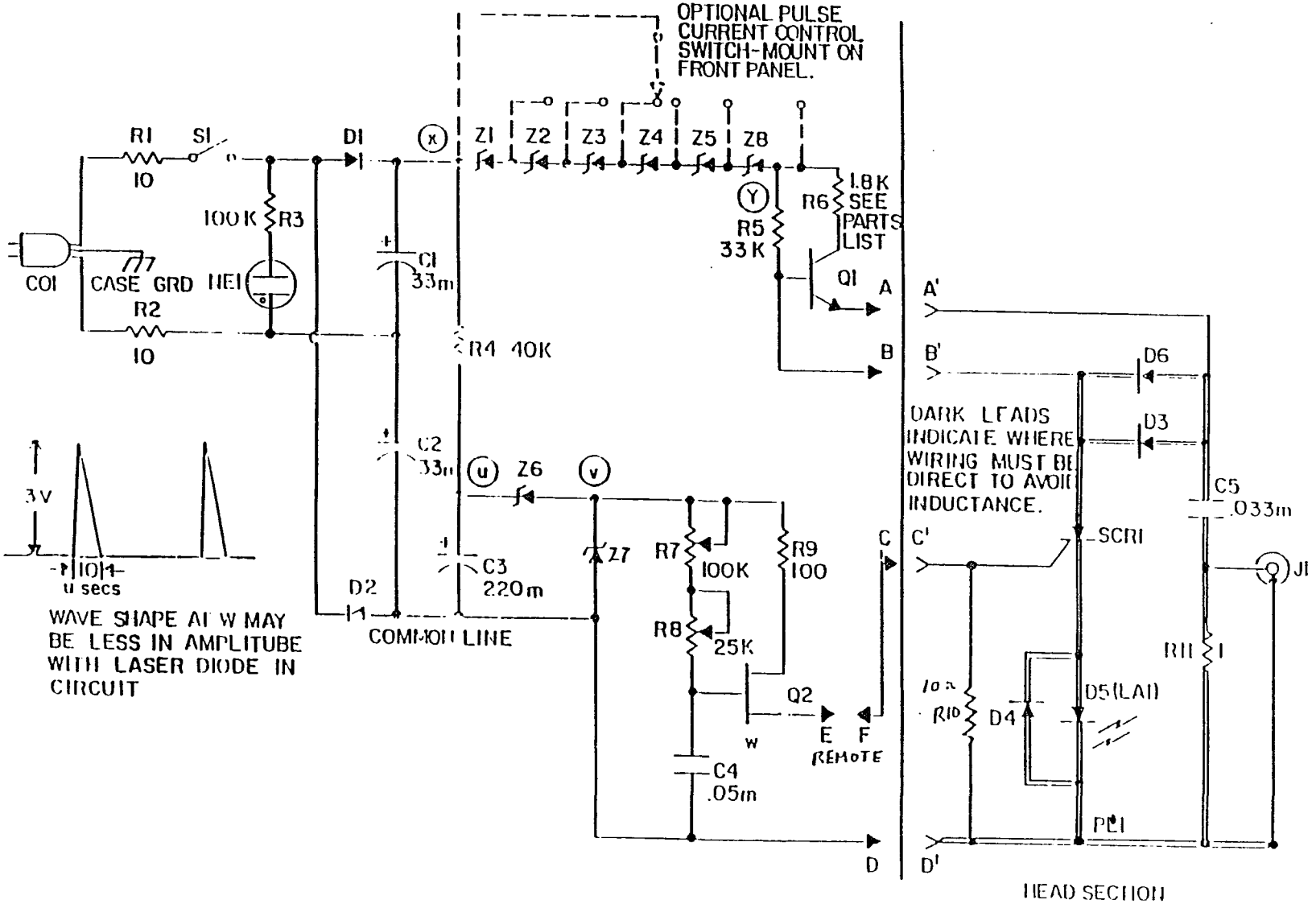

Figure.14 Power Supply and Pulser

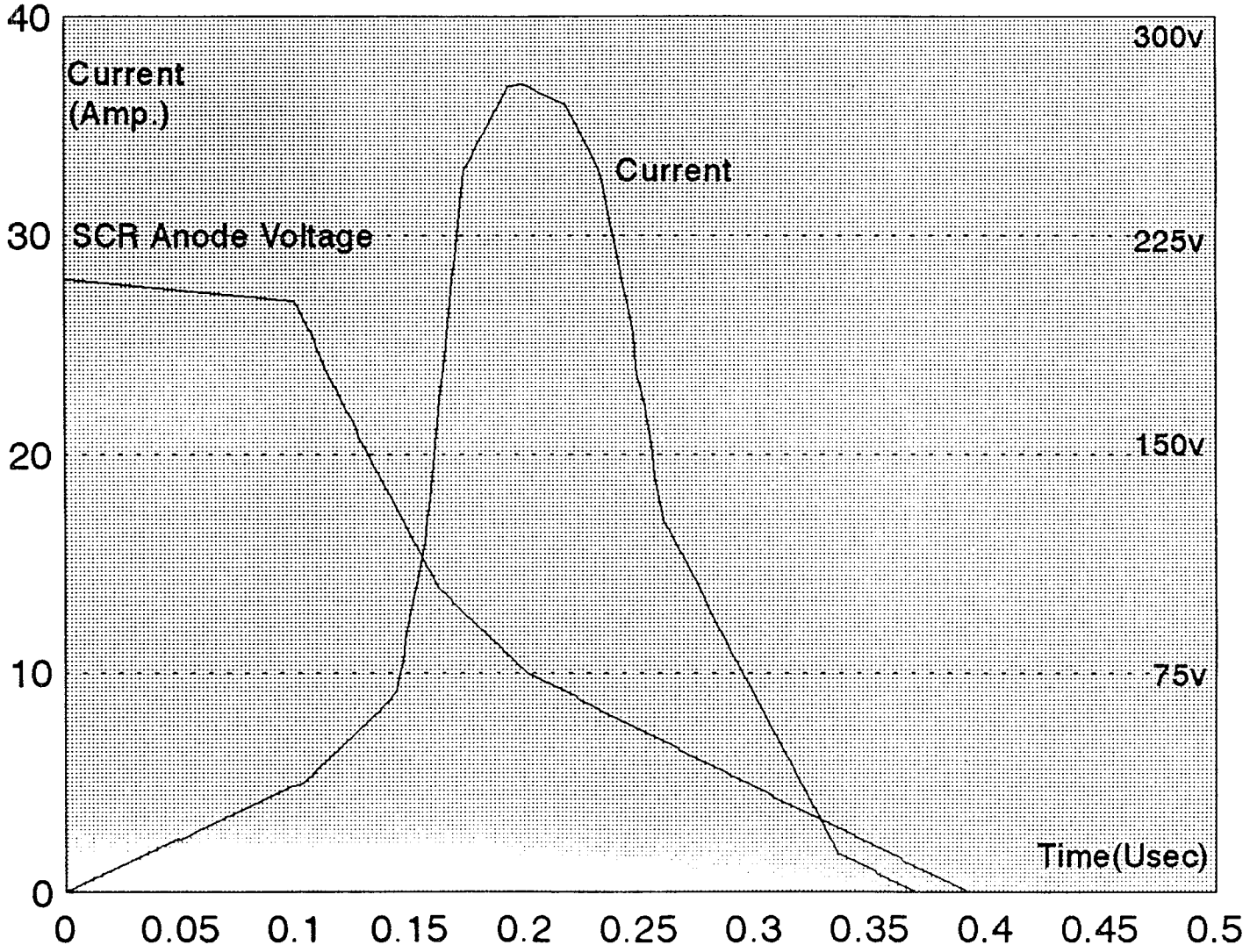

Figure.15 SCR Voltage/Peak Current

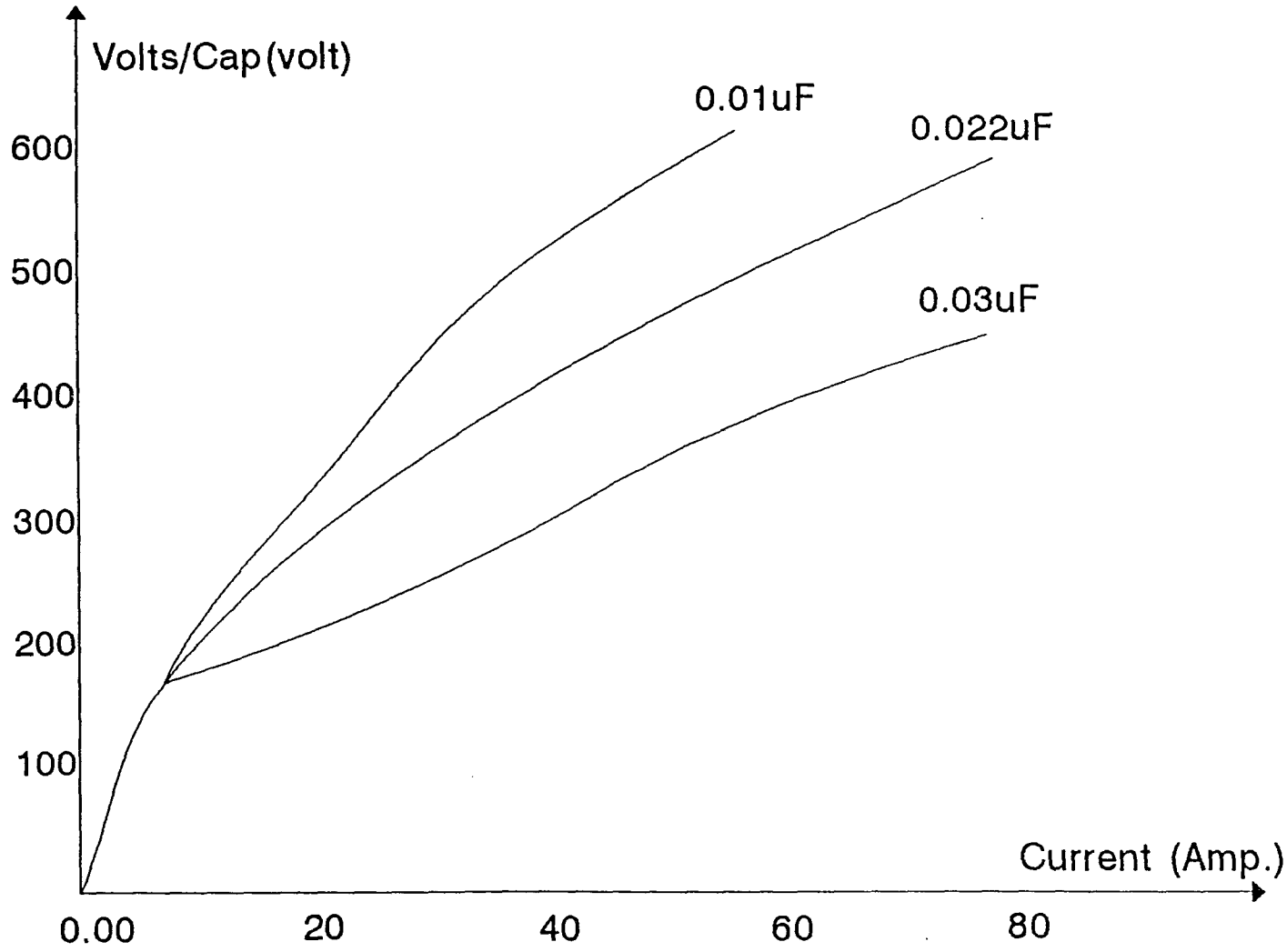

Figure.16 Current/Volts Per Cap

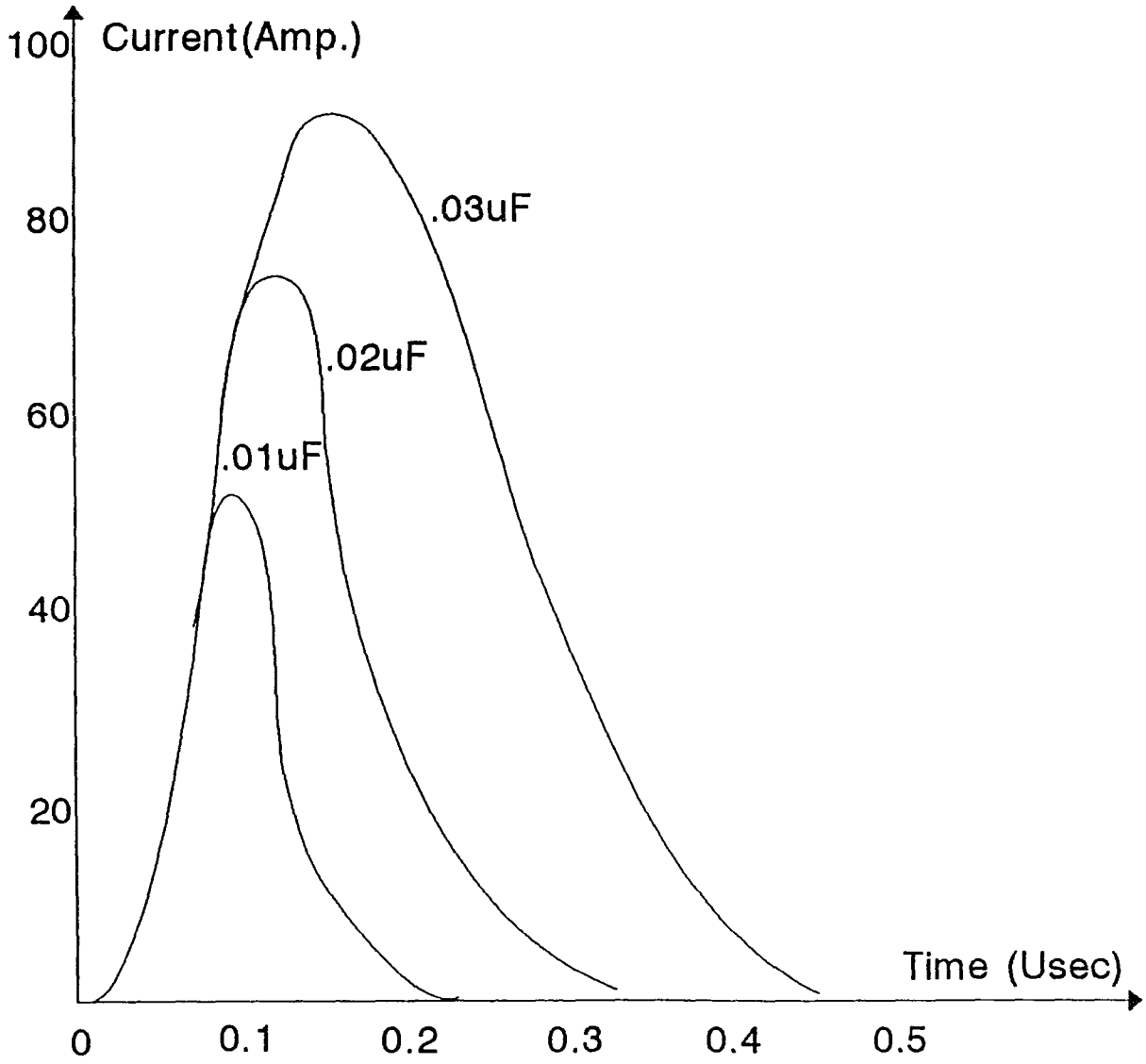

Figure.17 Peak Current/Cap Values

(a): Photodiode Cross-Section

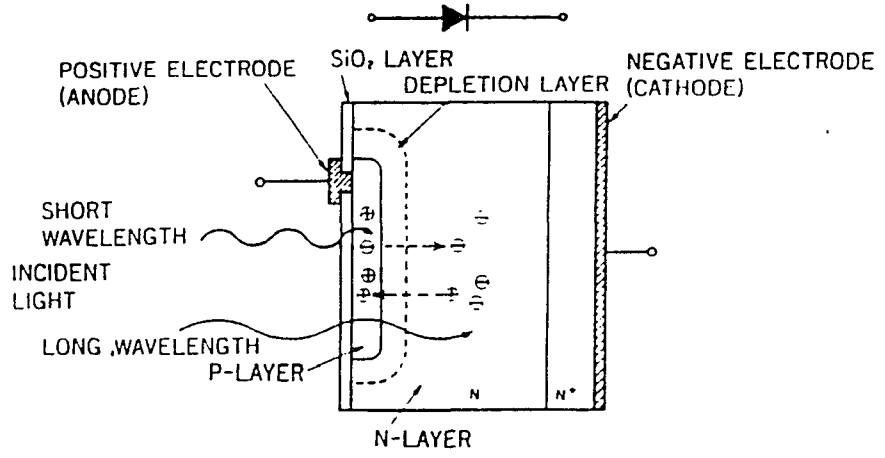

(b): Photodiode P-N Junction States

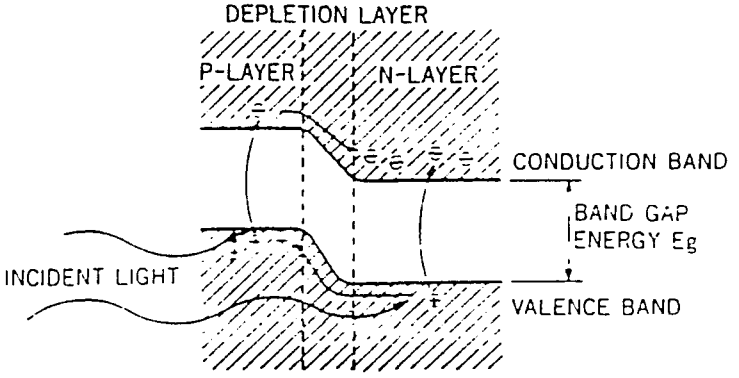

Figure.18

Photodiode Cross-Section and P-N Junction

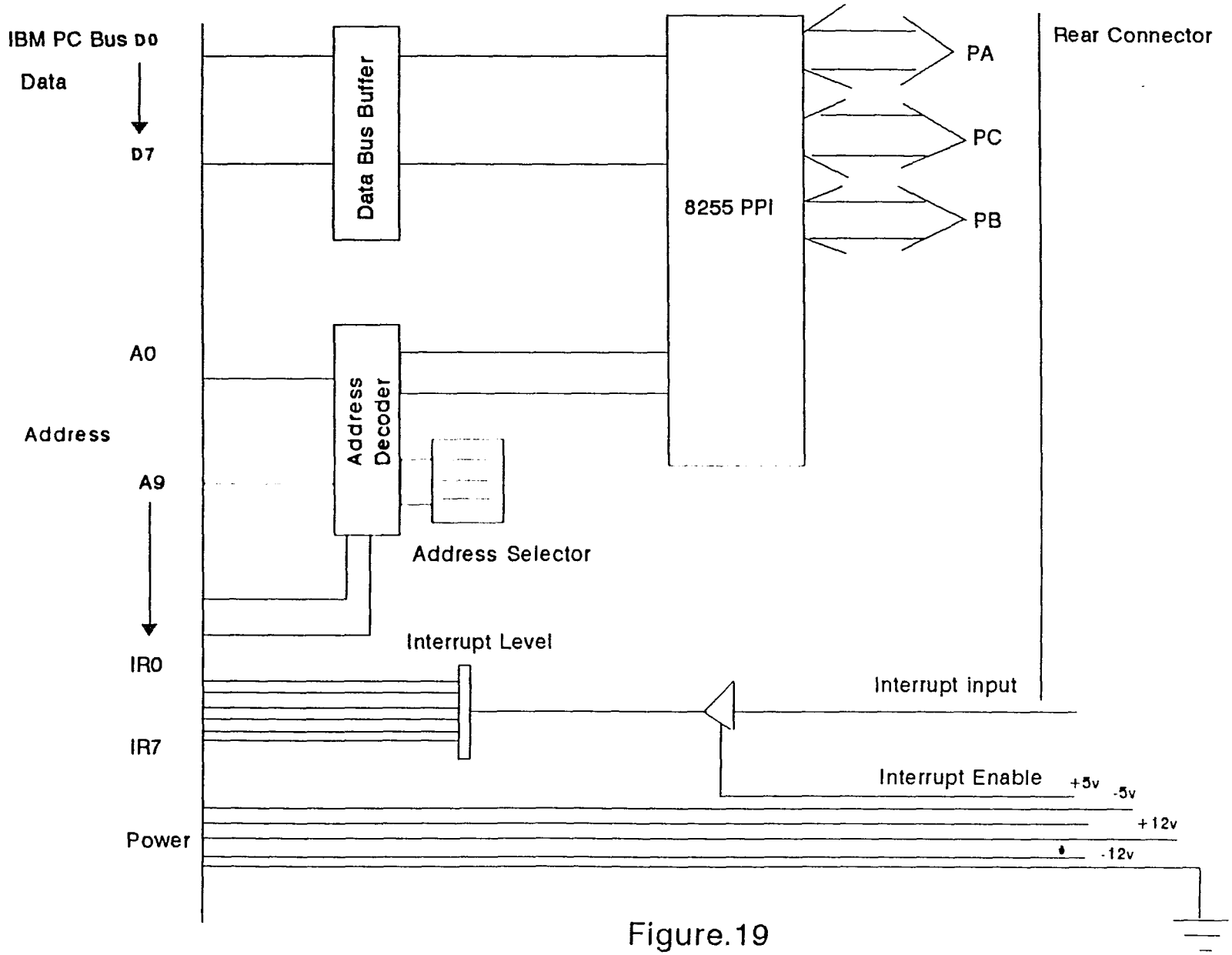

Figure.19

Parallel Digital I/O Board Block Diagram

CHAPTER 4

SYSTEM EXPERIMENTATION AND EVALUATION

4.1 Calculation of Signal to Noise Ratio:

The overhead infrared active-laser vehicle detector system must achieve a signal-to-noise ratio (SNR) which is sufficient to ensure a high probability of detection with a low false alarm rate. The SNR which yields a probability of false alarm of one per 1000 pulses for a range of 18m can be calculated following the analysis in[22]. The calculation yields a required voltage SNR of 7 or a power SNR of 17dB. This means that we must have minimum SNR of 17dB to insure the detection of vehicles.

We now must calculate the laser range SNR to ensure it exceeds 17dB. This requires knowledge of the received signal and background power. The received background power can be calculated using the equation:

$$P_B = L_\lambda A_R \Omega_R \Delta\lambda T_R T_F e^{-\sigma R} \qquad (4.1.1)$$

where $L_\lambda = PE_\lambda/\pi$ is the spectral radiance of the background/vehicle due to the reflected solar radiation, P is the background/vehicle reflectance, E_λ is the spectral solar

irradiance, A_R is the receiver aperture area, $\Omega_R=\theta_I\theta_1$ is the receiver solid-angle FOV, θ_I and θ_1 are the receiver angular field of views (FOV) in directions parallel and perpendicular to the diode laser junction, $\Delta\lambda$ is the optical filter bandpass, T_R is the receiver lens transmission, T_F is the optical filter transmission, σ is the atmospheric extinction coefficient, and R is the range to the vehicle which can be determined by using the same analysis in[23&24].

The received signal power can be calculated from the equation[25]:

$$P_s=LA_R\Omega_R T_R T_F e^{-\sigma R} \qquad \textbf{(4.1.2)}$$

where $L=P_vE_T/\pi$ is the radiance of the vehicle due to the diffusely reflected transmitter radiation, P_v is the vehicle reflectance, $E_T=P_{T_e}^{-\sigma R}/R^2\Omega_T$ is the transmitter irradiance at the vehicle, P_T is the peak power exiting the transmitter aperture, Ω_T is the transmitter beam solid angle, and the other symbols are as previously defined. For beam-filling target where $\theta_R>\theta_T$, θ_R is determined by θ_T and $\theta_R/\theta_T=1$.

The SNR is given by the equation:

$$SNR = \frac{P_s^2 R_0^2}{(2qP_b R_0 + i_{na}^2)\,\Delta f} \qquad \textbf{(4.1.3)}$$

where R_0 is the photodiode responsivity, q is the electron charge, $i_{na}{}^2$ is the amplifier mean square noise current per unit bandwidth, and Δf is the noise bandwidth. This is the ratio of the square of the signal current to the sum of the squares of the background noise current and the amplifier noise current. The silicon PIN photodiode we are using has a responsivity of 0.45 A/W at 900 nm. The low noise, high-speed, differential transimpedance amplifier has a rms noise current i_{na} of about 15 $pA/Hz^{1/2}$.

The parameter values required to compute the SNR are readily available, except for reflectance, which is the ratio of reflected to incident flux. Values of vehicle reflectance can be obtained from appropriate tables. Vehicle reflectance for black (0.5%) and silver-gray (27%)[26].

Equation (4.1.3) was used to calculate the SNR as a function of range for the following parameter values: P_B=0.3, E_λ=0.075w/$cm^2.\mu m$, θ_I=0.203rad, θ_1=0.005rad, A_R=1 cm^2, $\Delta\lambda$=0.04μm, T_R=0.9, T_F=0.8, P_T=50W, σ=0.125km^{-1}(standard clear day), R_0=0.45 A/W, i_{na}=15 $pA/Hz^{1/2}$, Δf=91.6MHZ, and P_v=0.005 and 0.27. Using

the above equations and values, plots of SNR versus range were obtained and shown in figure 20. The intersection of each curve with the 17dB line indicates the maximum range capability of the device detection. We found that for the worst case, for black vehicle, the SNR is 18dB for a distance of 18m. For the case of silver-gray vehicle, the SNR was close to 55dB for the same distance as shown in figure 20, while the SNR for the reflected signal from the road surface was 13.8dB, (no vehicle passing). Other curves for different colors vehicles are located between these two curves. Therefore, the system will be able to detect the passing vehicle under the worst case.

4.2 WEATHER EFFECTS:

For the system to operate very accurately, the effect of weather (rainfall, fog..etc) on the vehicle sensor performance must be taken into account. These performance can be demonstrated by calculating the minimum visibility at which the sensor can operate[27]. Since sensor operation is predicted upon detecting a return signal from the roadway, it will be assumed that the limiting condition for sensor operation is the detection of the laser pulse reflected from a surface of 10% reflectance (appropriate for macadam). Using the equations above to calculate the received signal power as a function of σ for a 10% reflectance and a nominal range of

10 m yields:

$$P_s=(1.53.10^{-5})e-20\sigma \qquad \textbf{(4.2.1)}$$

This can be equated to the value of P_s needed to achieve a SNR of 17dB, as calculated from equation (4.1.3), to yield $\sigma=0.156m^{-1}$. The visible extinction coefficient σ_v corresponding to 900 nm extinction coefficient (0.156 m^{-1}) can be obtained from the value(1.39) of the ratio of σ_v to the 900nm σ obtained from the plot of σ versus wavelength in figure 7-3 in [26]. As we knew that the extinction coefficient can be related to the visibility through the expression:

$$\sigma_v=3.912/R_v \qquad \textbf{(4.2.2)}$$

where σ_v is the average extinction coefficient for the visible spectrum and R_v is the visibility ranges. Therefore, this equation can be used to determine the visibility for any range.

This analysis indicate that the overhead infrared vehicle sensor will continue to sense vehicles until heavy fog/rainfall reduces the visibility range to 18 m. This suggests that a measurement of the return-signal amplitude can be used to ascertain the existence of poor highway visibility

conditions. This capability could be put to good use in warning freeway drivers to slow down because of dangerously low visibility conditions ahead.

4.3 BACKGROUND NOISE POWER:

Radiation incident on the photodetector is caused by reflection of the sun's irradiance at the vehicle and by scattered sunlight in the atmosphere between the vehicle and the receiver. The spectral solar irradiance M for the wave length 907 nm is $0.045 W/cm^2\mu$ under normal atmospheric conditions with the sun at its zenith[23]. At night time the irradiance was measured to be $6.10^{-9} W/cm^2\mu$. The total received background noise power can be calculated using equation (4.1.1).

Equation (4.1.1) describes the contribution of noise power due to reflected background radiation at the vehicle. The vehicle fills the receiver beam and acts as reflector. The equation also gives the amount of background radiation that is scattered in the atmosphere, between the receiver and any vehicle, toward the receiver. The determination of this quantity of radiation is difficult because of the variability of the atmosphere and the dependance of scattering on the relative angle of the sun and the receiver line of sight. For purposes of calculation, the scattering is assumed to be

isotropic with the volume scattering coefficient equal to the atmospheric extinction coefficient neglecting absorption.

Typical noise voltage was 3 mV peak-to-peak on a bright day. This was measured by blocking the receiving lens and observing the decrease in noise voltage. The mean squared noise current i_n^2 is given by[28]:

$$i_n^2=2q\Delta f(Q_0P_B+Q_0P_s+i_d)G^{2.3}+i_{na}^2 \qquad \textbf{(4.3.1)}$$

Where q=electronic charge, Δf=receiver bandwidth, Q_0=unity gain responsibility=0.62A/W, i_d=dark current=15 pA, λ=wave length, h=Planck's constant, c=velocity light, G=valanche gain, $G^{2.3}$=approximate excess noise factor due to avalanche process and i_{na}=amplifier noise current=$3.2\text{x}10^{-9}$A. Therefore, for a gain of 100dB, we obtain the root mean square(rms) noise voltage, V_n:

$$V_n=i_nR_L \qquad \textbf{(4.3.2)}$$

i_n was determined from equation 4.3.1, ($i_n=0.66\text{x}10^{-7}$ A), R_L=2000Ω, therefore the rms noise voltage becomes:

$V_n=0.66\text{x}10^{-7}\text{x}2000=1.32\text{x}10^{-4}$ mV.

4.4 PROGRAMMING FOR VISUAL DISPLAY OF STATISTICS FOR MOVING VEHICLE:

Programs are written in C and Assembler languages that allow for visual display of statistics for moving vehicles and determine the cross-correlation functions[29]. These programs control the PIO-12 interface card and display the relationship between traffic flow and time.

A bydata's interface card is installed inside the PC workstation. This card is inserted in the slot (8) on the Workstation motherboard. We set bit "0" of PA as our input. Each time a vehicle passes under the laser beam, the receiver will receive an interrupted signal which is transferred to the bit "0". This interrupted signal represents one count in this program.

The C program has many segments. The first segment sets the graphic screen and builds the coordinate axis. The second segment receives the data through the interface card and plots the curve of traffic flow vs. time. The third part collects the same data and produces the statistics of traffic. The data to be collected include the arrival time, number of passing vehicles, their speed and their length. These statistics are expected to be useful in observing and managing the traffic.

But the most important program is the Assembler one. This program uses the received real time data, interrupted and uninterrupted signals(due to a passage of vehicle) to calculate cross-correlation function. These data are the output of the A/D convertors. By finding the cross-correlation functions T_x and T_Y, then T_d can be determined. These are necessary for the calculation of the speed and the length of the passing vehicle.

4.5 EXPERIMENTAL RESULTS:

An experimental prototype system was built and was tested in both the laboratory and in the field in at least six separate tests for vehicle counting. Each field test lasted between 2-4 hours. For field testing the prototype was mounted on a pedestrian bridge over a main street in the CCNY Campus in upper Manhattan. The system readily detected passage of cars, vans, trucks, motorcycles and pedestrians under a variety of conditions. Different vehicle colors had no impact on the counting and accuracy of the system.

4.5.1 Effects Of Vehicle Passage On Reflected Signal:

Figure 21 shows the typical laser signal transmitted by the system and detected at street level. Figure 22 shows the corresponding signal reflected from the street and detected at

the overpass and amplified further. It is this received signal that is affected/ interrupted by the passage of vehicles. The interrupted signal from a clear roadway remains essentially constant. It may, however, undergo gradual changes in amplitude due to reduction in visibility (fog etc). Abrupt changes are due to passage of vehicles. Figure 23 shows the effect on the received signal as a van passes through the laser beam footprint on the roadway. Figure 24 shows effect of the passage of a vehicle. The reflected signal received from the van is stronger because of the van's height and hence shorter distance to the detector. In addition the duration of the reflection disruption, is related to the length of vehicle. These results were found typical for vans and cars over many tests. In general reflected signal were consistent and readily interpretable.

The effects of cloudy, rainy and humid conditions were also checked. There were no significant impacts. No test measurements were carried out in fog, since there were no foggy days during the field tests. It should be noted, however, that the signal-to-noise ratios typically obtained with the system were over 50dB. This meant that even a several hundred-fold reduction in signal due to fog could be tolerated and the system would still operate satisfactory. (A several hundred fold reduction in visibility would also probably mean no traffic could circulate).

As described above, the detection system incorporated an automatic gain control amplifier (AGC). Thus, as the received signal is diminished due to deteriorating visibility, the receiver gain is automatically increased to compensate and ensure that the detector system output is essentially unchanged for the counting and signal -processing stages. Road surfaces covered with a layer of snow would have no detrimental effect on the system since all they would do is enhance the steady state signal. Falling snow would result in an increase in the noise in the system as reflections are obtained from individual flakes. However, with the 1khz tuned detector approach (which could be easily increased to 10khz) this effect is expected to be negligible.

4.5.2 Vehicle Counting Tests:

Figure 25 shows the results for 80, 90 and 120 minutes of operation of the counting system, during which 39, 40 and 110 vehicles passed respectively. A vehicle passage is represented by a step jump in signal. Absence of vehicles is represented by a straight line. Results of tests were checked, and vehicle counting corroborated by human visual observation.

In general, test results demonstrate that the sensor system reliably detects and counts vehicles. Typically counting errors were less than 0.5%, in vehicle samples of

over 200. These errors occurred either because of the low S/N ratio, below 17dB, or because of the passage of vehicle out of the field of view. Vehicles which stopped in between the two laser beams could be detected by the interval between a count on the first beam reflection and that due to the second. Additional tests are now underway to check and evolve the speed and length measurement capabilities of the system based on the cross-correlation approach described above. The results of this work will be reported in a subsequent paper.

A prototype has been built to test the technical feasibility of the system. It has been tested in the Laboratory as well as in the field. A site has been selected on Campus for field testing. The prototype system has been mounted on a pedestrian bridge over the main street on Campus. The system detected passage of small vehicles, vans and pedestrian accurately.

4.5.3 Effect Of Humidity :

Tests were performed for different humidity conditions. Figure 26 shows the effect of humidity the received signal strength. It is clear that the humidity has no effect on the performance of the system.

4.5.4 Cross-Correlation :

A simulator has been built to verify the cross-correlation capability of the system. The cross-correlation function $R_{xz}(k)$ is calculated and plotted versus k (i.e. number of pulses). The solid curve in Figure 27 shows $R_{xzo}(k)$ which represents the case of no vehicle passing. Other curves represent $R_{xz}(k)$ when a vehicle interrupts the detector. Therefore, when a vehicle passes under the first beam, the auto-correlation function will be calculated between the two signals Z(k) and X(k)to determine T_x, at the same time when the same vehicle passes under the second beam, the auto-correlation function will be calculated between the two signals Z(k) and Y(k) to determine T_Y. T_x and T_Y will used to determine the time T_d which is necessary to calculate the speed of the vehicle. Figure 26 also shows the case when a bird or any sort on noise picked up. In this case the auto-correlation function will be determine and then will go back , to the case of no vehicle passing due to the discontinuity of the information that provided to the sensor.

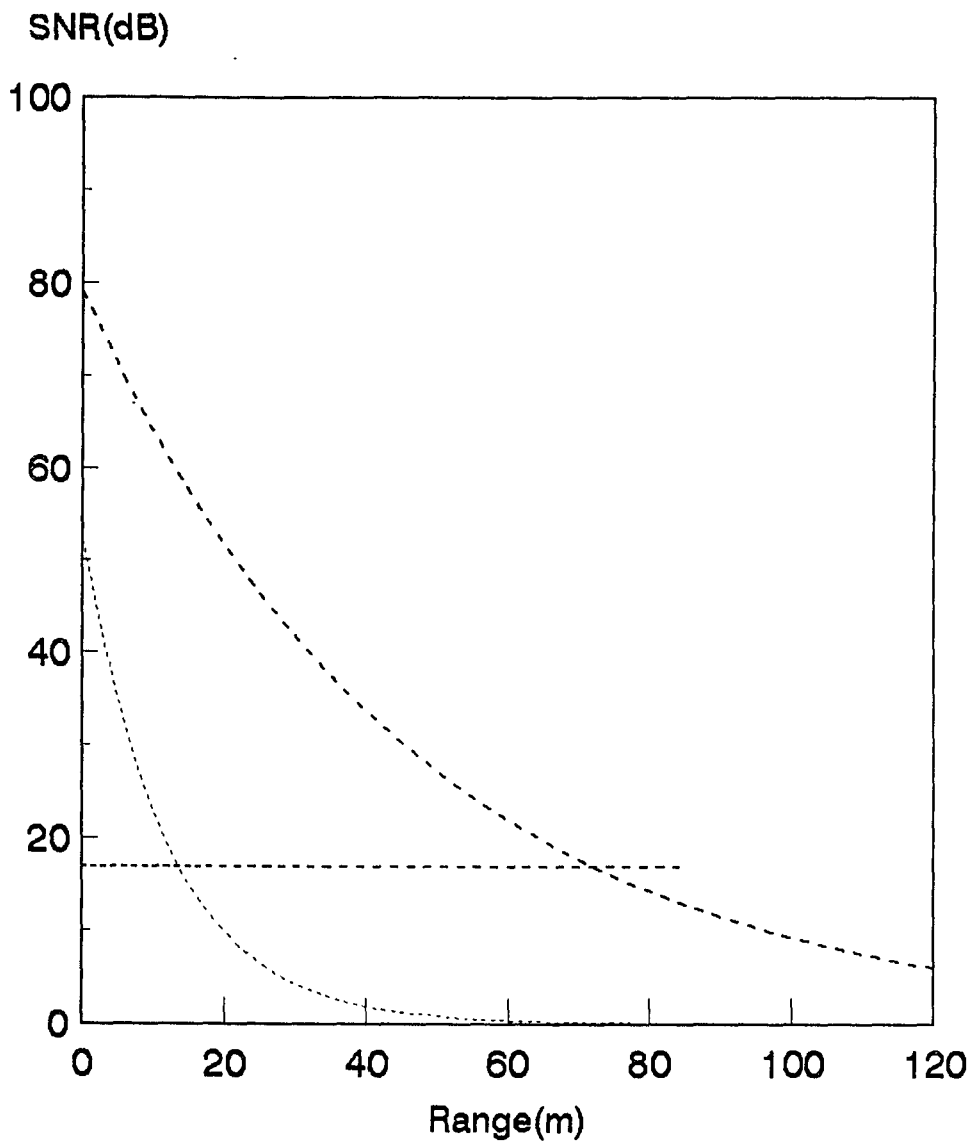

Figure.20
Reflected Power From Different Vehicles of Different Colors

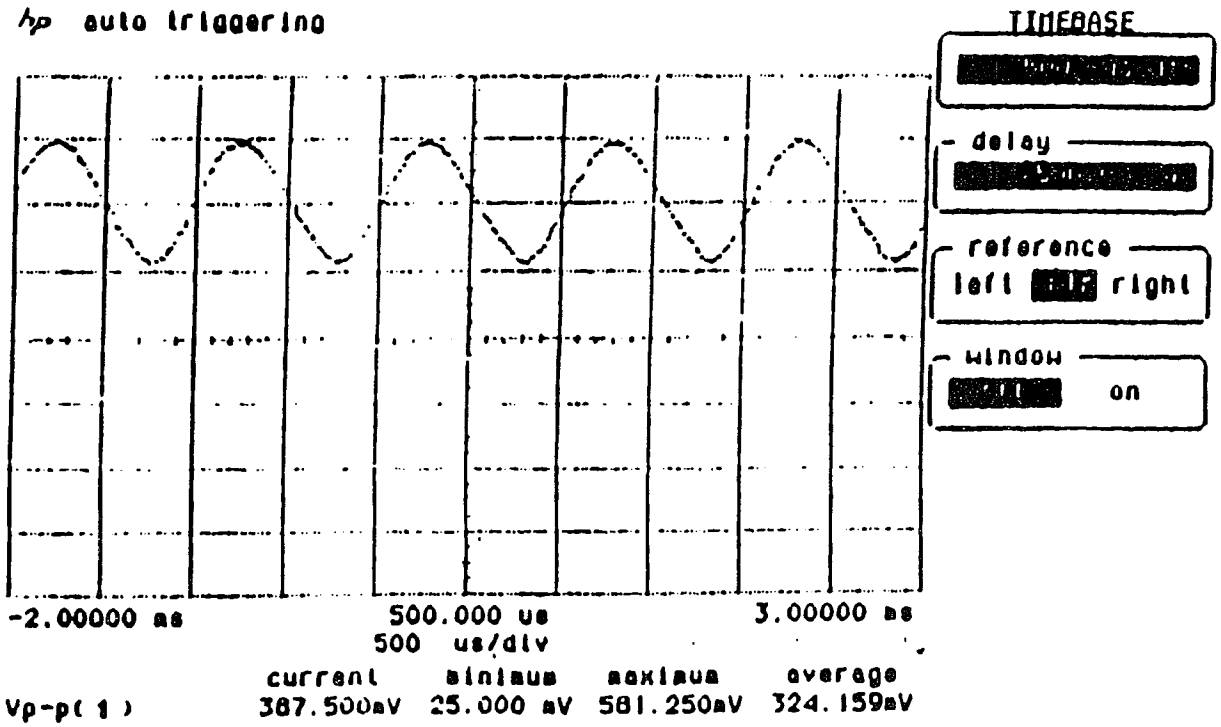

Figure.21 Transmitted Signal

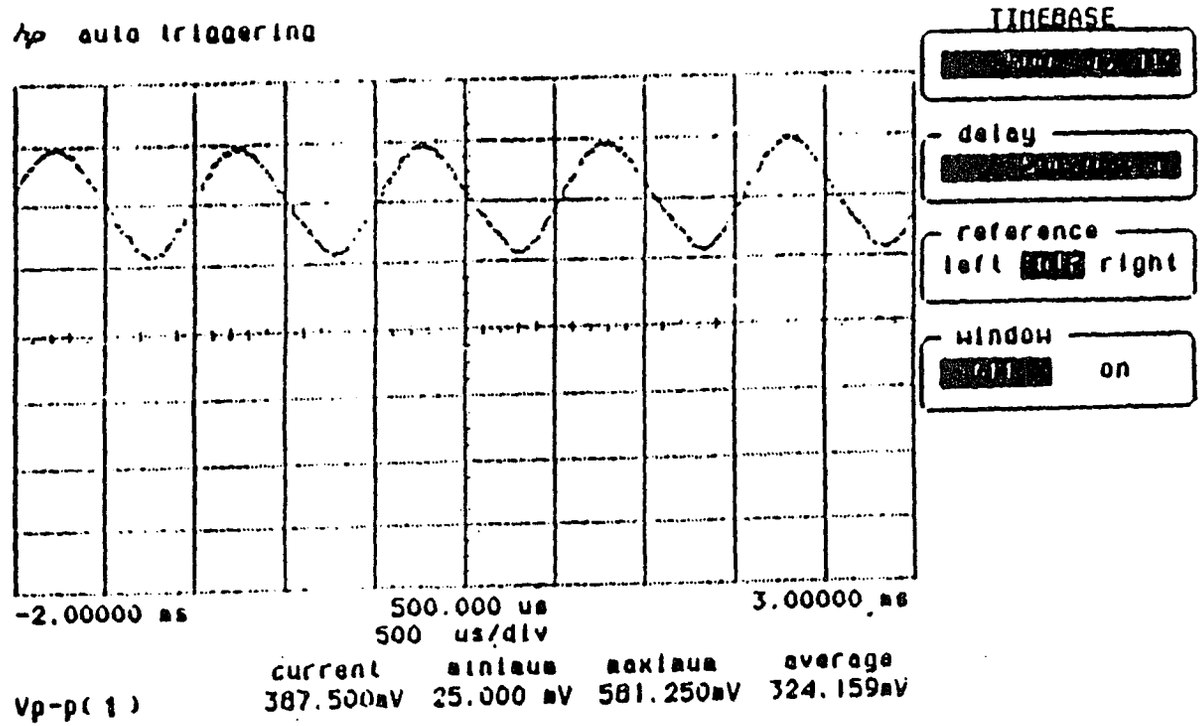

Figure.22 Received Signal

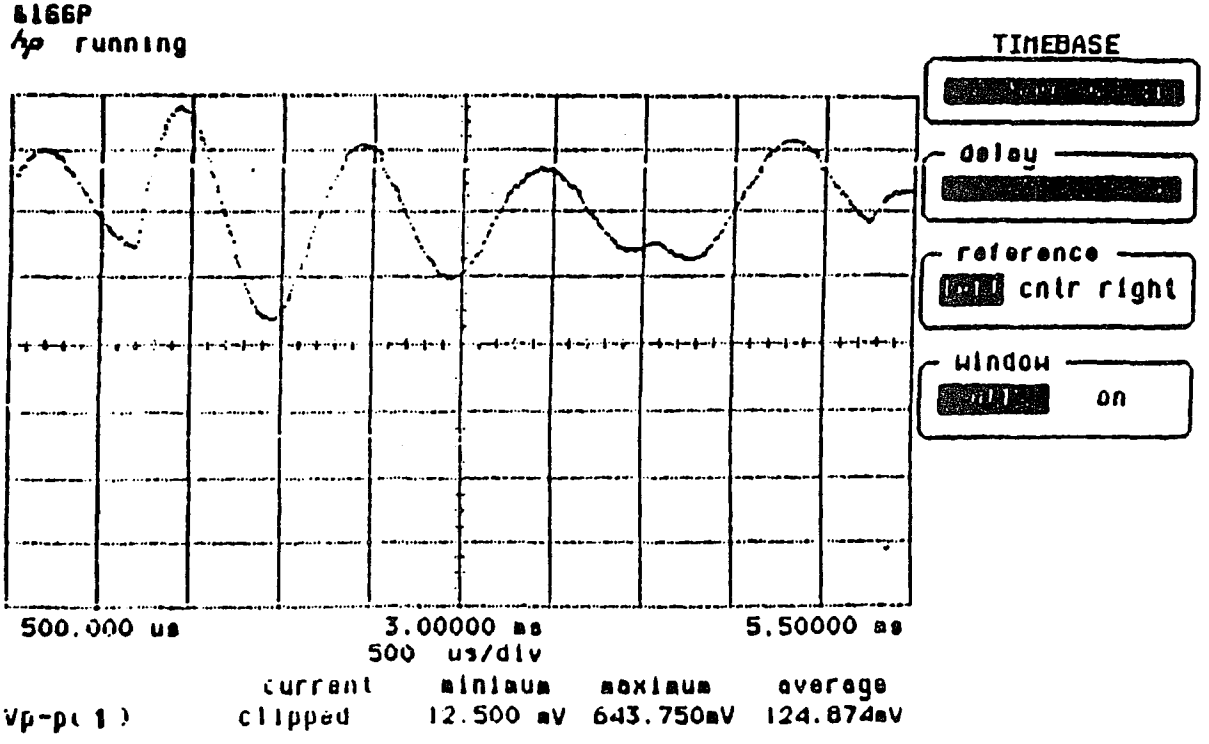

Figure.23

Reflected Signal from a Surface of a Van

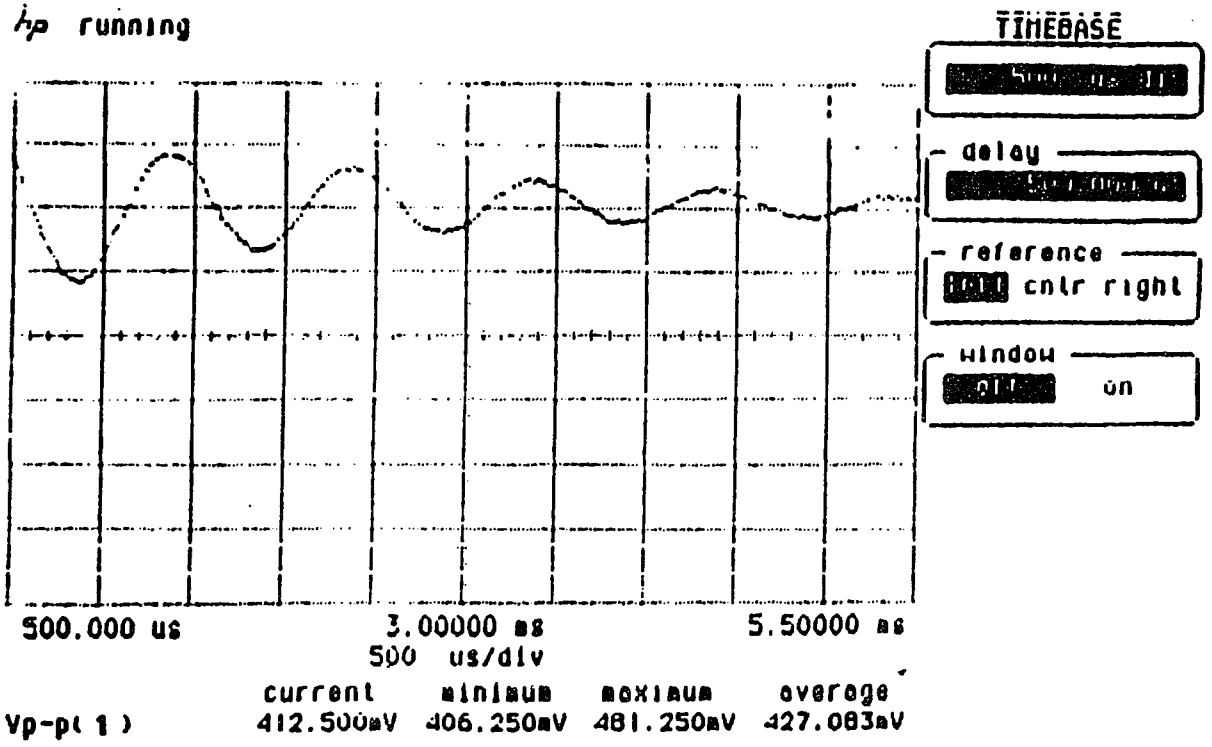

Figure.24

Reflected Signal From a Surface of a Car

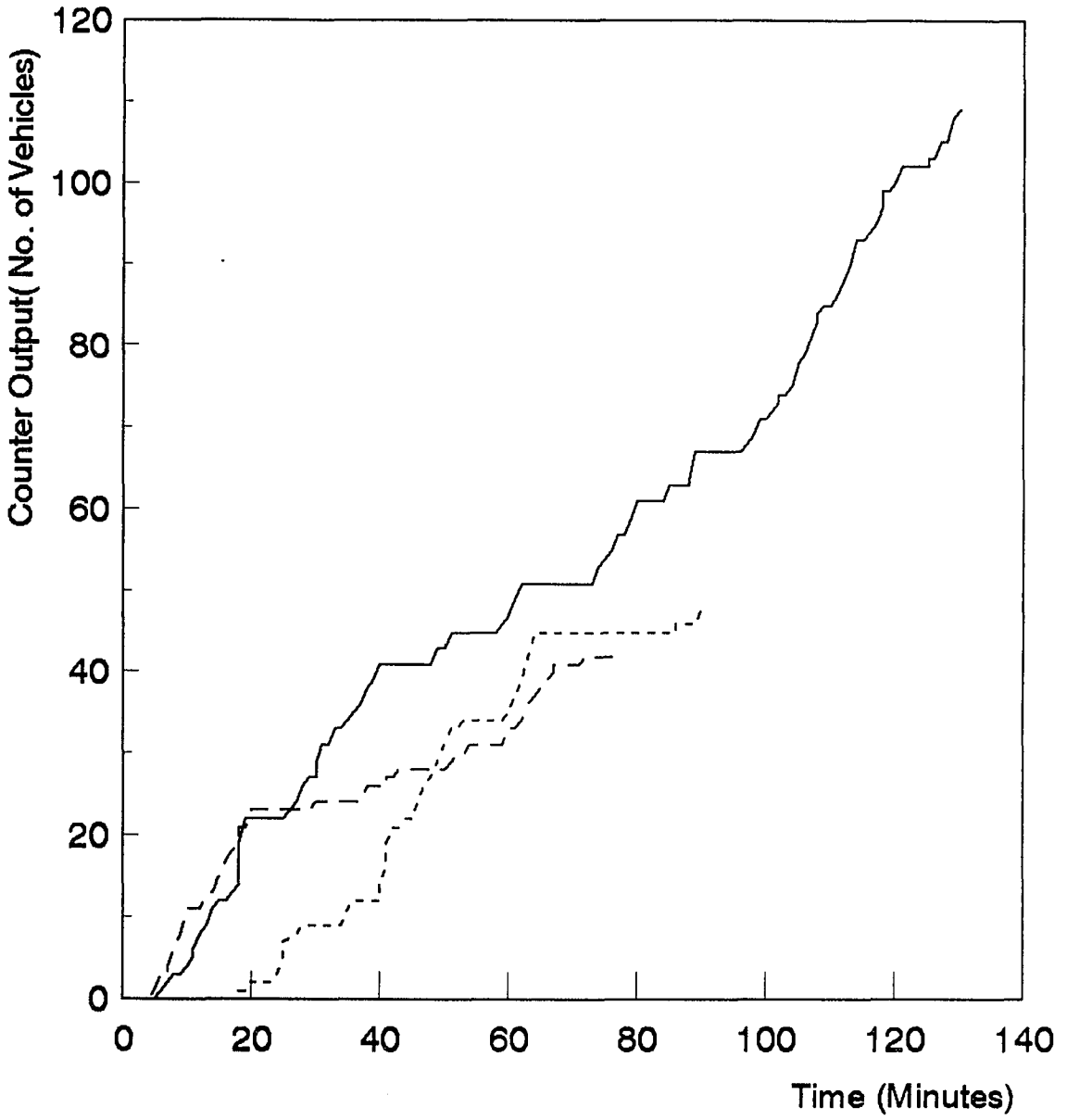

Figure.25
Computr Display of Vehicle Counting

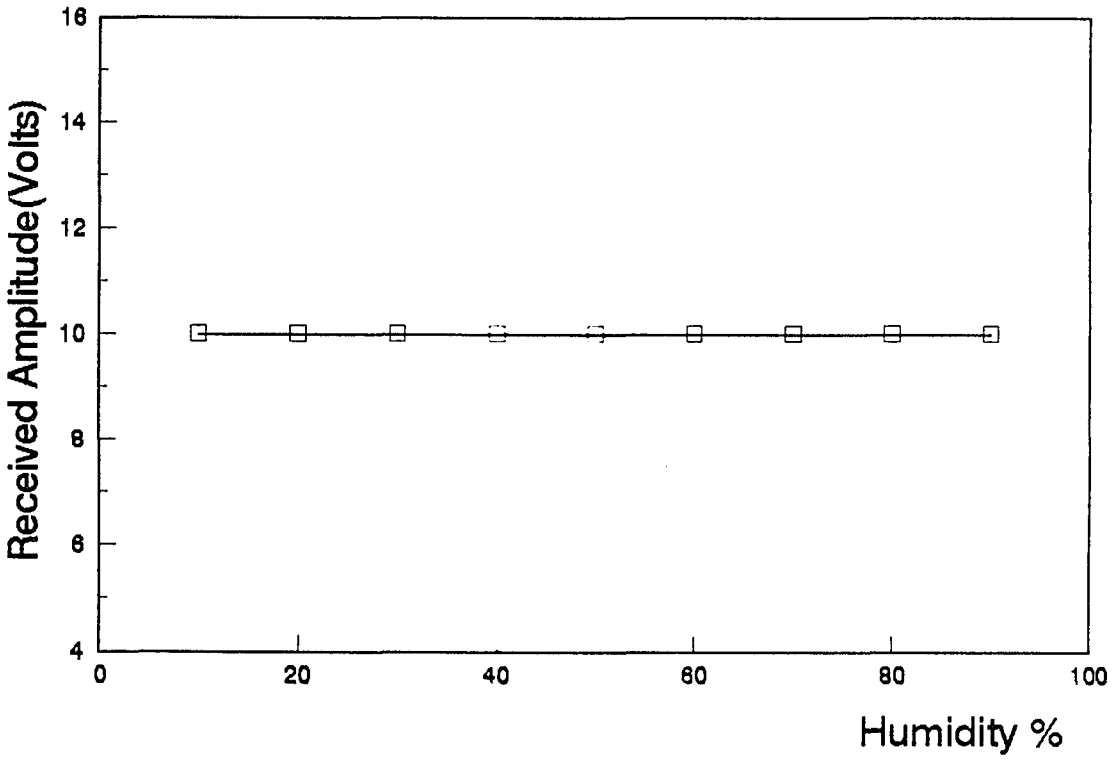

Figure.26
Effect of Humidity on the Signal strength

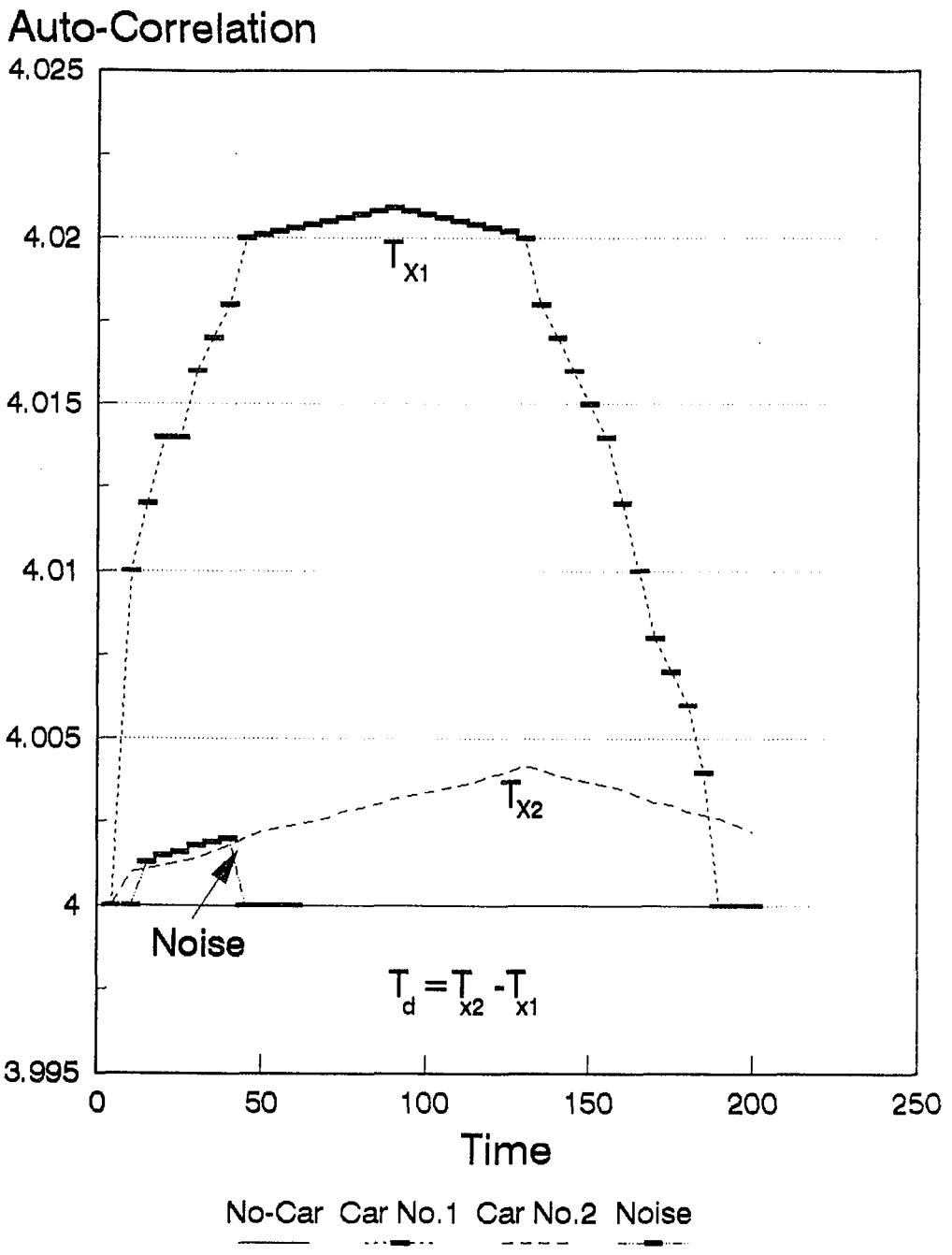

Figure.27
Cross-correlation Function

CHAPTER 5

CONCLUSIONS AND FUTURE RESEARCH

5.1 Conclusions:

The basic elements of a system using infrared lasers and computerized correlation techniques to monitor and detect road vehicles was successfully developed and demonstrated in the laboratory. Preliminary road tests with the laboratory equipment confirmed the basic capabilities of the system. The results of this work indicate that a product based on the system technology developed shows promise of being a practical cost effective device.

This approach is intended to demonstrate and determine different specific capabilities in field operations and the prototype parameters required to achieve them. The information obtained can then be used to assess the potential scope for use (and hence potential market) for the different possible configurations, as well as provide some indication of the likely production costs of each. This information is needed so that potential manufacturers can assess the attractiveness of entering this business and producing the sensors being developed in this thesis.

5.2 Future Research :

It is important to exploit these results and develop a feasibility prototype which can be used to optimize parameters for a variety of vehicle monitoring applications and to evolve prototype parameters including portability, raggedness, and the use of low cost components. Based on this, our system parameters can be designed to be compatible with traffic counting and control equipment. Feasibility prototypes with these characteristics can be built and laboratory and field tested, and parameters optimized in conjunction with feedback to be obtained from Traffic Control. In these field tests, the parameters of the feasibility prototype systems will be refined and designs optimized. Based on these optimized designs, and their achieved field performance, it will then be possible for a potential manufacturer to properly analyze costs and other commercial production concerns and market potential that need to be determined prior to commercial production being sensibly embarked upon.

We recommend four stages as future follow-ups.

1. Review and Modification of our System Parameters in Context of Desired State-of-the-Art System Parameters.
2. Design and Construction of Feasibility Prototype.

3. Laboratory Tests and Optimization.
4. Minimizing Errors Rate, (this can be done by expanding the illuminated area by the optical transmitter, so that at road surface it lies across an entire lane).
5. Field Test-Final Optimization and Evaluation.

It is also important to apply different technologies for the same system to obtain closely results. During the previous few months, we designed and built a pyroelectric system which has the capability to detect and monitor traffic[30]. This device is an passive detector (with out active laser transmitter). It was tested in the campus at The City College of New York. The field tests results proved that the system is capable to detect and monitor vehicular traffic. Therefore, it is very important to modify this passive system for more sophisticated measurements like speed and length of vehicles and probably vehicle identification which becomes one of the main factors in IVHS during the recent time. In the following sections, we will give a complete description on the passive (pyroelectric) sensor.

5.2.1 Pyroelectric Sensors (Passive Detectors):

Before we start describing the passive sensor, we would like to give an idea about this type of sensor and how it operates.

5.2.2 Pyroelectric Sensor (Detector):

Since the resistance of most semiconductors is a strong function of temperature, the resistance of most semiconductor chip can tell us how much radiant energy is falling on it. Such a device is very sensitive, relatively rugged, and can detect radiation over a very wide spectral range. Pyroelectrics are thermal sensor of this type. Its response is independent of the wavelength of light or radiant energy it receives, a fact that makes the device useful from anywhere in the spectrum between and including soft X-rays to the far infrared. Yet, the pyroelectric is especially practical for the mid to far infrared because of its high sensitivity without the need for cooling.

In these sensors the thermal infrared optical power is converted to an electrical output. They can provide up to 4 orders of magnitude higher output signals than thermopiles, making the pyroelectric much easier to interface with a measurement or control circuit. Moreover, the pyroelectric

responds only to a change in radiation intensity. And it is easier detecting a change than discriminating a small shift in levels[31].

5.2.3 Passive Infrared Traffic Monitoring System:

5.2.3.1 System Elements

The basic elements of the system consist of two passive (pyroelectric) detectors S1 and S2. Each pyroelectric sensor consists of a window, a semiconductor sensing element, and integral built in electronics[31]. The window restricts incoming radiation to thermal infrared, 10 micron wavelength band of interest. The semiconductor responds to the incident energy changing its resistance and the built in electronics converts this into a usable output signal, typically in the 100 millivolt range. The window which is sealed protects the semiconductor and built-in electronics from physical damage and moisture. The two detectors are mounted on lamp standards or other elevated structures above the roadway so they have a line of sight to the approaching traffic on the lane they are monitoring, see figure 28.

when vehicle passes in the field of view of a detector, its passage will cause significant change in the received signal picked by the pyroelectric sensor. This signal will be compared to the steady state signal (no vehicle signal) for

the purpose of counting. For a simple counter any significant change in the received signals X(k) and Y(k) that are picked up by sensors S1 and S2, (See figure 29), with respect to the steady state signal, no vehicle, can be used to detect and count passing vehicles.

For velocity measurements and vehicle characterization, it is necessary to consider the time the vehicle takes to traverse the distance (d in figure 28) between footprints of the fields of view of the two sensors on the roadway. Since the distance d is fixed the delay, T_d, between the two points T_{x0} and T_{y0} which represent the time at which signals X(k) and Y(k) start changing with respect to the steady state signal (see figure 29) will depend on the speed of passing vehicle, and can in principle be used to measure it. The actual interruptions in the steady state signals, T_x and T_y, in each of the received signals depend on the speed and length of the vehicles as they pass through each of the sensor field of view footprints on the roadway. Therefore, knowledge of T_x, T_y and T_d can be used to determine speed, acceleration and length.

5.2.3.2 Vehicle Counting:

For simple counting of vehicle's passage, it is only necessary to record and count the episodes when the received

signal by undergoes an abrupt and sustained change from the normal steady state signal. It is, however, important that the circuitry and logic doing that be capable, through proper programming, of distinguishing changes in the received signal (from the steady state)caused by the passage of vehicles from that caused by other spurious interruptions (such as that caused by a bird flying across the field of view). Figure 30 shows a block diagram of the system arrangement used for simple counter. The pyro-electric sensor responds to a change in detected thermal radiation intensity such as that produced by a passing vehicle. The detected signal is converted to an electric output. This output signal is then interfaced to the electronic processing circuitry. The signal received is typically in millivolt ranges. It is passed through a comparator block. The comparator uses mirror opamps to compare the received signal output from the detector, when a vehicle passes, with the steady state signal. Opamps chosen for this purpose have common mode rejection ratios (CMRR's) of the order of 60 dB. These high CMRR's permit the Opamps to respond only to the difference signal. The difference signal is then amplified.

The optimum gain setting for the Opamp depends on the thermal background noise, which are in turn dependent on the aperture and field of view generally needed to restrict detection for the passage of one vehicle at a time. For 50-60

meter detection distances typically required for vehicle monitoring, a gain of 40 dB on the Opamp was found to result in acceptable signal to noise ratios (over 100:1) for vehicle passage detection.

In the system used, high voltage difference signal signifies the presence of a vehicle and steady signal (0v difference signal) signifies absence of vehicles. This difference signal is fed into a RCA555 chip to generate a series of pulses, see figure 31. These pulses are fed into a programmer delay block. This block consists of 3 synchronous programmable counters are used to set-up the counter threshold and are controlled by a microprocessor. A clock frequency of 1 KHz is generated using monostable multivibrator to drive these counters to operate synchronously. Each counter gives a pulse to the next one after it completes its counting. Each counter counts from 0-15, Each bit count is 10 nsec. For if a counter starts counting from 0 the maximum delay will be 160 nsec. But if it starts from some arbitrary number it will count up to 15 (e.g. if a counter starts counting from 13, then the delay period will be 20 nsec only). An algorithm is constructed to control the timing of the pulse. Then the output signal of the programmed counters is fed to a decade counters then to displayed to show the actual counting.

5.2.4 Practical System Parameters:

The monitoring system using infrared pyroelectric detectors is designed to be low maintenance and easy to install. Approximate cost estimates call for $150 in material and labor in quantity production. This may be compared to installed loop costs of $1800-$3200 plus disruption of traffic during loop installation.

The system needs to have sufficient sensitivity to give satisfactory signal-to-noise ratios in order to be reliable and effective. To optimize signal-to-noise ratios, an infrared passive detector with build in amplifier and band pass filter is used. It also has optics covering only the clearly delineated zone where the vehicles are expected to pass. The signal comparator used in this system has several advantages. It not only compares the received signal with the reference signal but it also provides amplification for ease of detection. There is also, a variable instrumentation amplifier to control both the amplification and the sensitivity. This permits tuned detectors to be used to reduce noise. That way it can be readily identified and differentiated from spurious signals.

The experimental system used is shown in Figure 32. Two pyroelectric detectors are used in conjunction with collimator

to cover two zones of detection on the road surface passing vehicles. The received signals due to the passage of a vehicle go into amplification stages and then to a counter and displayer to count and show the number of passing vehicles. The amplifier output can also be fed to subsequent signal processing steps for speed and length determinations measurements.

5.2.5 Experimental Results:

An experimental prototype system was built and was tested in both the laboratory and in the field in at least seven separate tests. Each field test lasted between 1-5 hours. For the first field tests the prototype was mounted on a pedestrian bridge over a main street in the CCNY Campus in upper Manhattan. The system was next tested at a cross-road in Syracuse NY, in collaboration with Traffic Control Technologies Inc. The system readily detected passage of vehicles, vans and trucks under a variety of conditions.

5.2.5.1 Effects Of Vehicle Passage On Received Signals:

Figure 33 shows the typical signal when there is no vehicle passing (steady state signal or absence of a vehicle). Figure 34 shows the received signal as a Van passes through the field of view. Figure 35 shows the passage of a Car. The

signal received from a van has wider pulse widths because of the van's length and hence longer time under the field of view of the sensor. These type of tests were carried out repeatedly and the results were consistent and readily interpretable. The effects of cloudy, rainy and humid conditions were checked. There were no significant impacts.

No test measurements were carried out in foggy conditions, since there were no locally foggy days when field tests were carried out. However, the signal-to-noise ratio typically obtained with the system was over 40dB. This means that even a several hundred-fold reduction in signal due to fog could be tolerated and the system would still operate. (Several hundred fold reductions in visibility would also probably mean no traffic could circulate).

5.2.5.2 Vehicle Counting Tests:

Figure 36 shows the results of field test at City College, New York, for 80, 90, 120 and 200 minutes duration. During these period 39, 44, 59 and 120 vehicles passed respectively. Figure 37 shows the results, of the field tests that were carried out in Syracuse in conjunction with Traffic Control Technologies Inc, for 2 and 4 hours duration. During these period 125 and 320 vehicles passed respectively. Vehicle passage is represented by a step jump in signal. Absence of

vehicles is represented by a steady (straight line) signal. Figure 37 shows the results of these field tests. These results are compared with measurements by a loop detector.

Figure 38 shows the recording on the control screen of the loop detector. **X** represents presence or passage of a vehicle, while a blank represents absence of vehicles. During these two test periods (2 & 4 hours) the pyroelectric detector detected 125 and 320 vehicles respectively. The loop detector covering the same lane detected 136 and 329 vehicles respectively. The reason for the differences in the results arises from the fact that the loop detectors count additional numbers of axles in case of truck passage. Results of tests were checked, and the vehicle counted by infrared system was corroborated exactly by human visual observation. The test results demonstrate that the sensor reliably detects vehicles.

Additional tests are now underway to check and evolve the speed and length measurement capabilities of the system based on the cross-correlation approach described above. I am also recommend that this passive system should be more developed and more tests should take place. I believe that the passive system will fit very well in most transportation applications because it is easy to install, cost-effective system and it does not need an FCC license to operate.

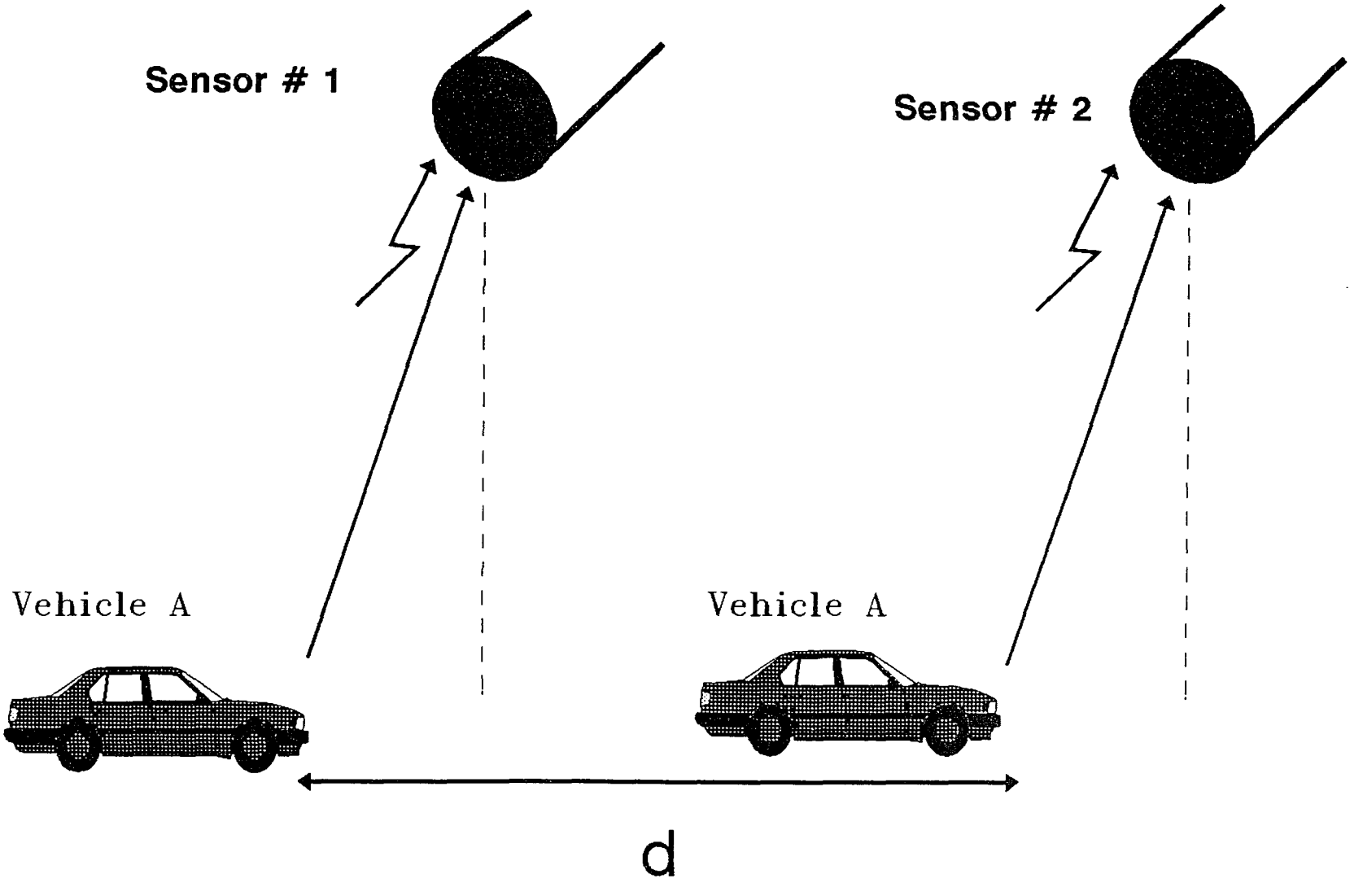

Figure.28 Physical Setup

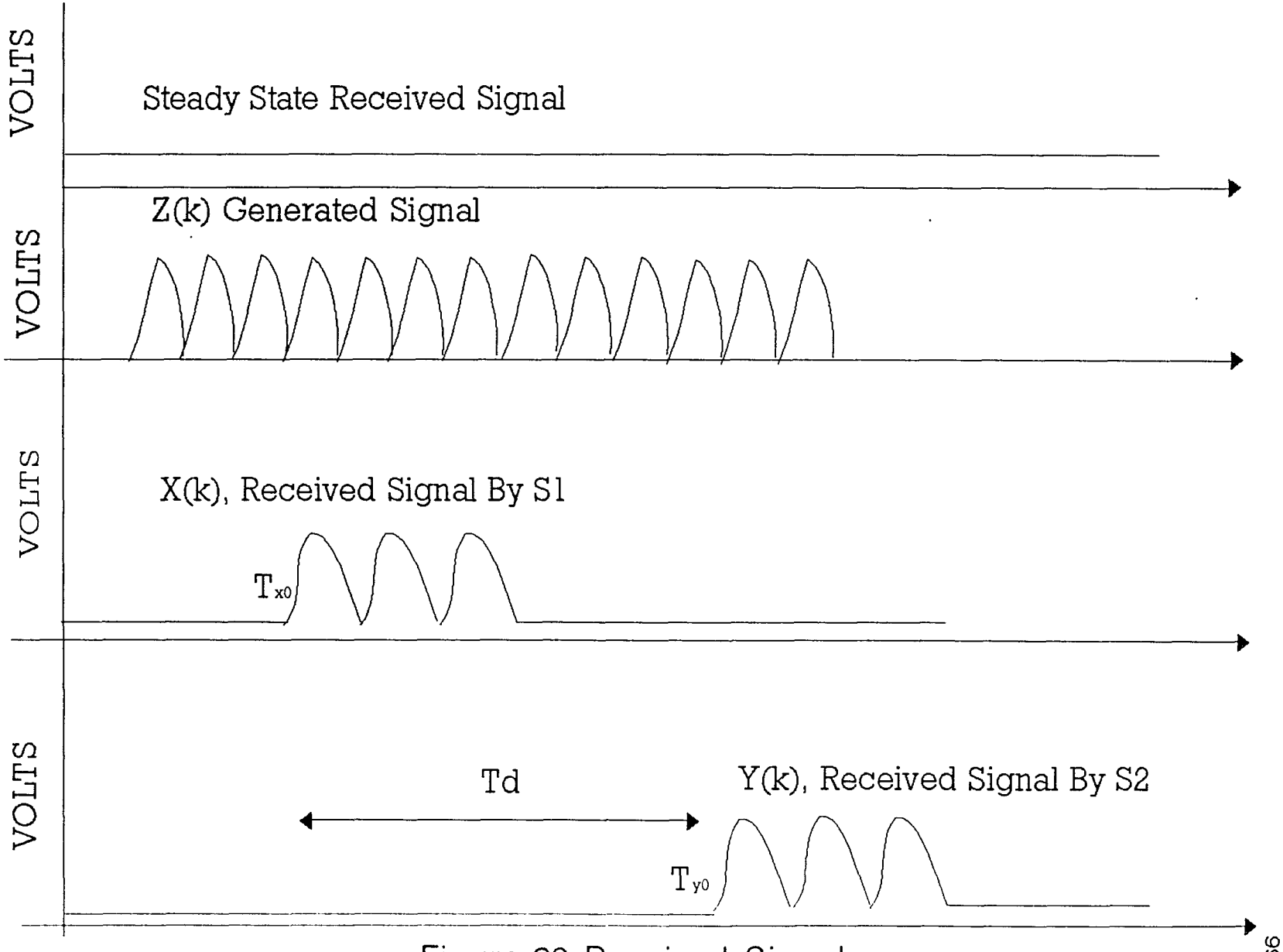

Figure.29 Received Signals

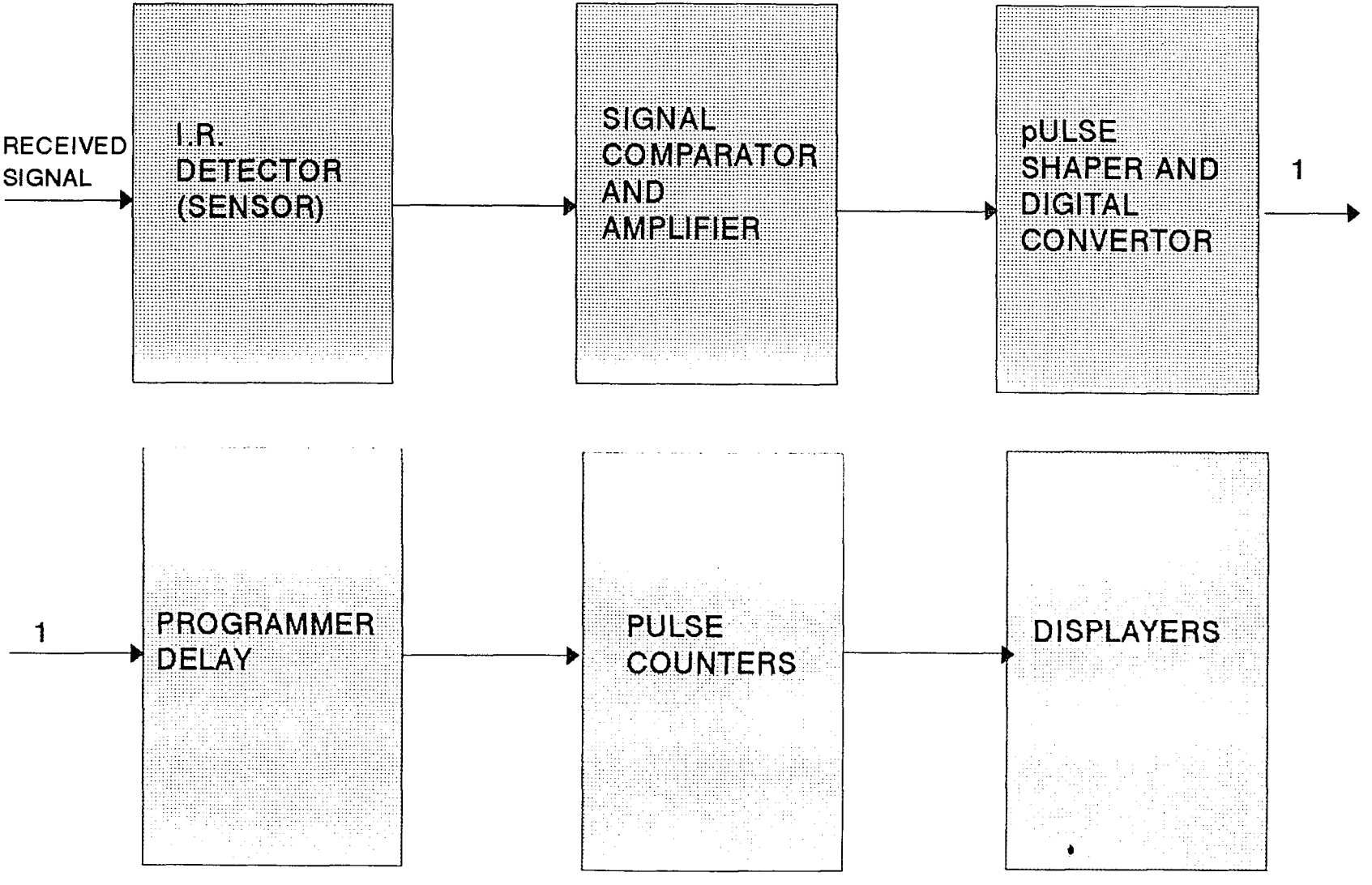

Figure.30 Block Diagram For Vehicle Counting System

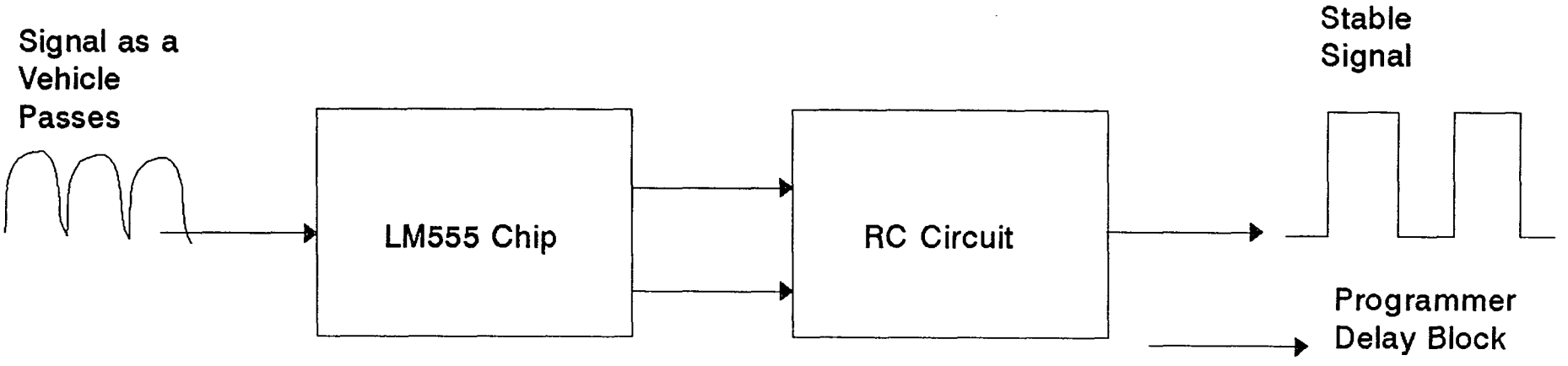

Figure.31
Signal Re-shaped Circuit

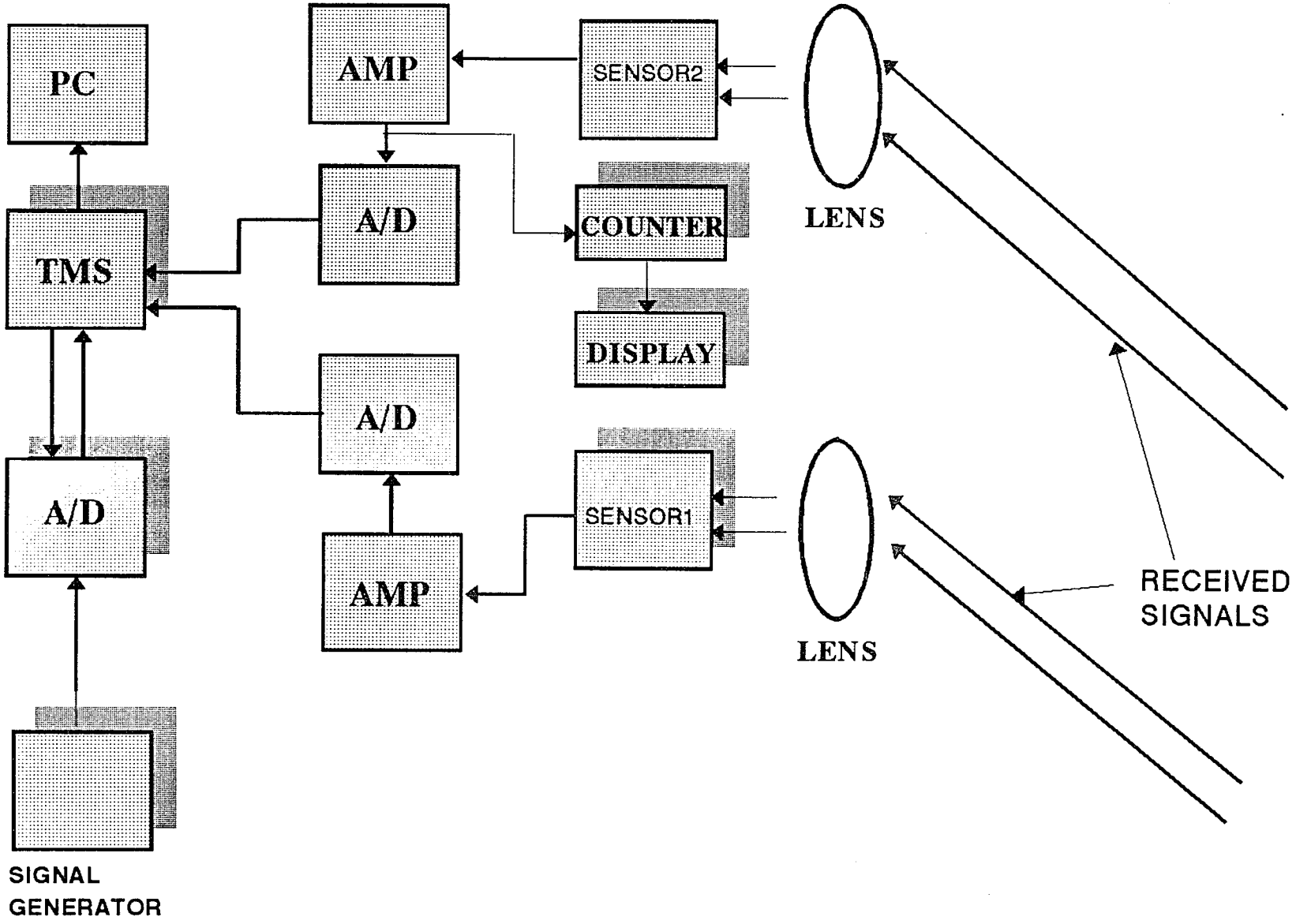

Figure.32 System Block Diagram

Figure.33 Steady State Signal (Absence of Vehicle)

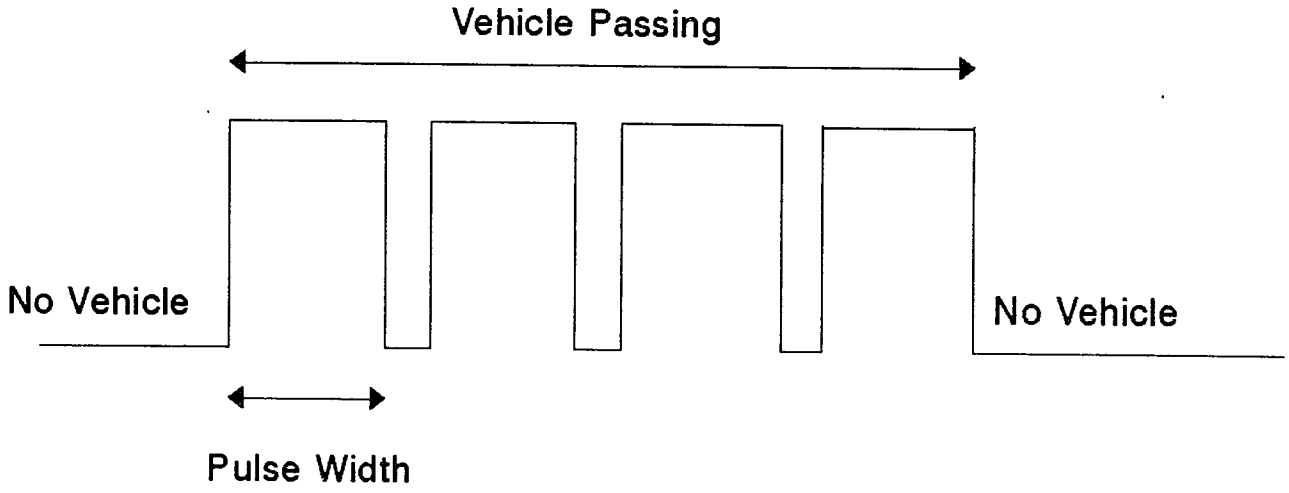

Figure.34
Received Signal as a Van Passes

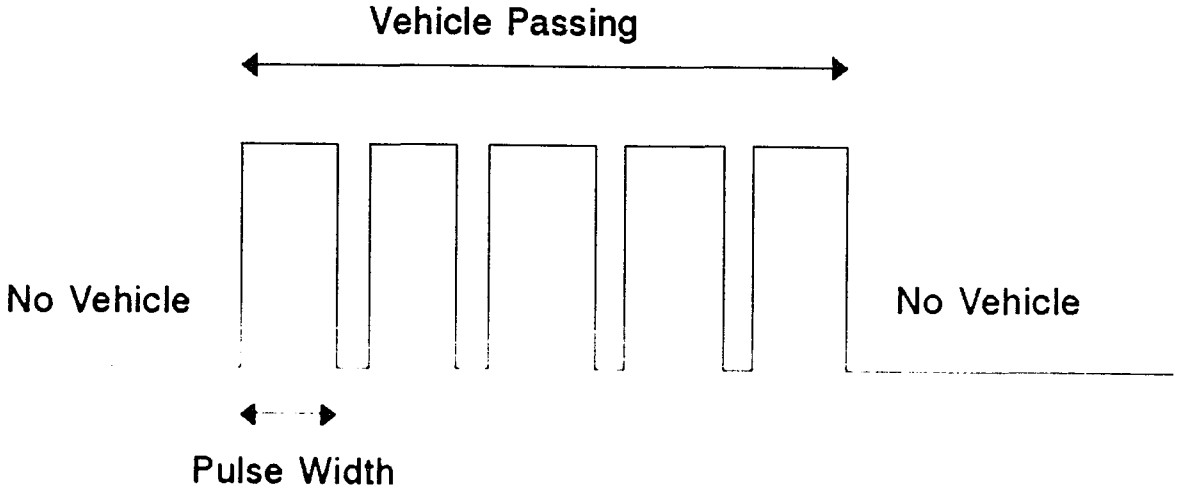

Figure.35

Received Signal as a Car Passes

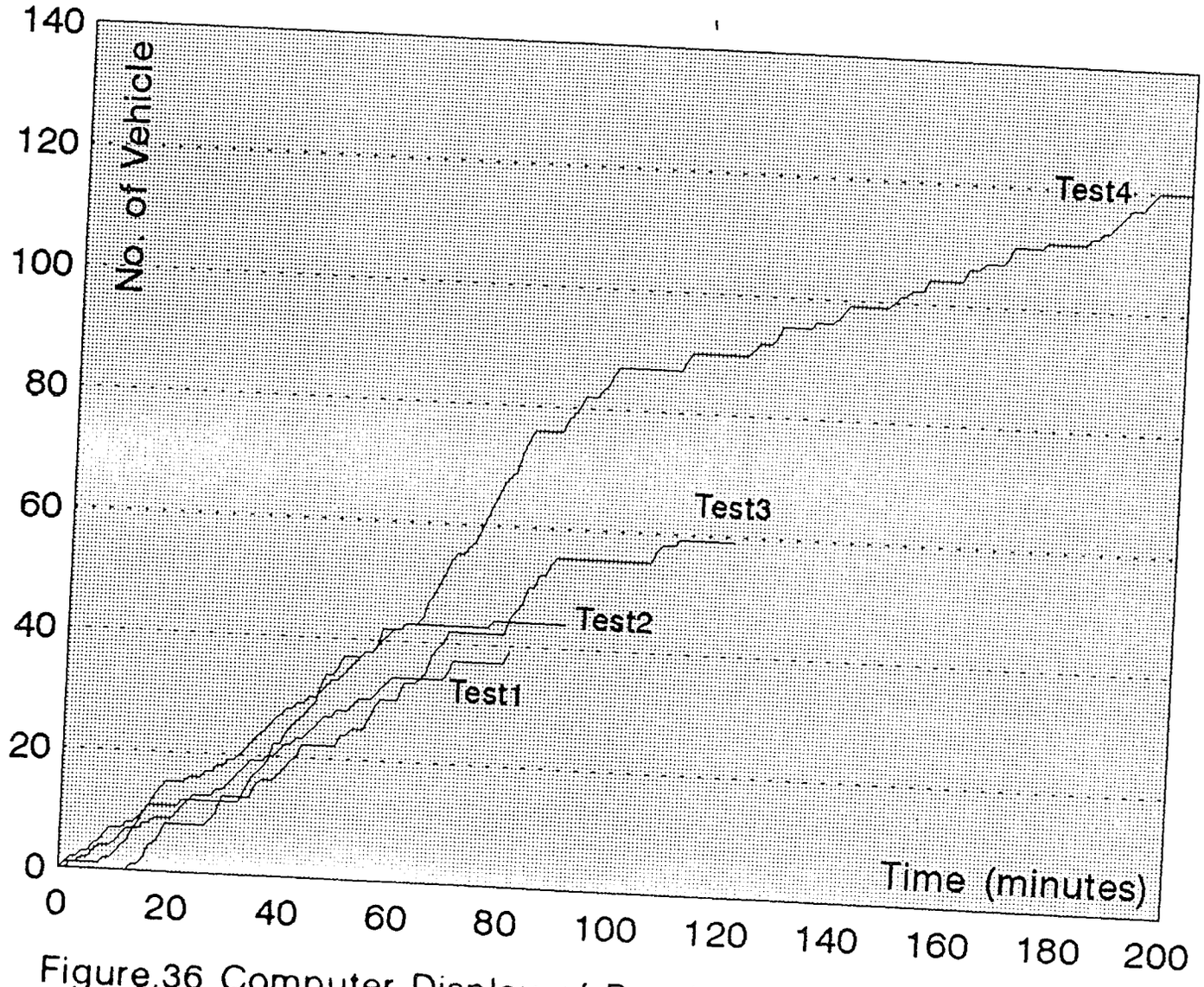

Figure.36 Computer Display of Passive System Field's Tests

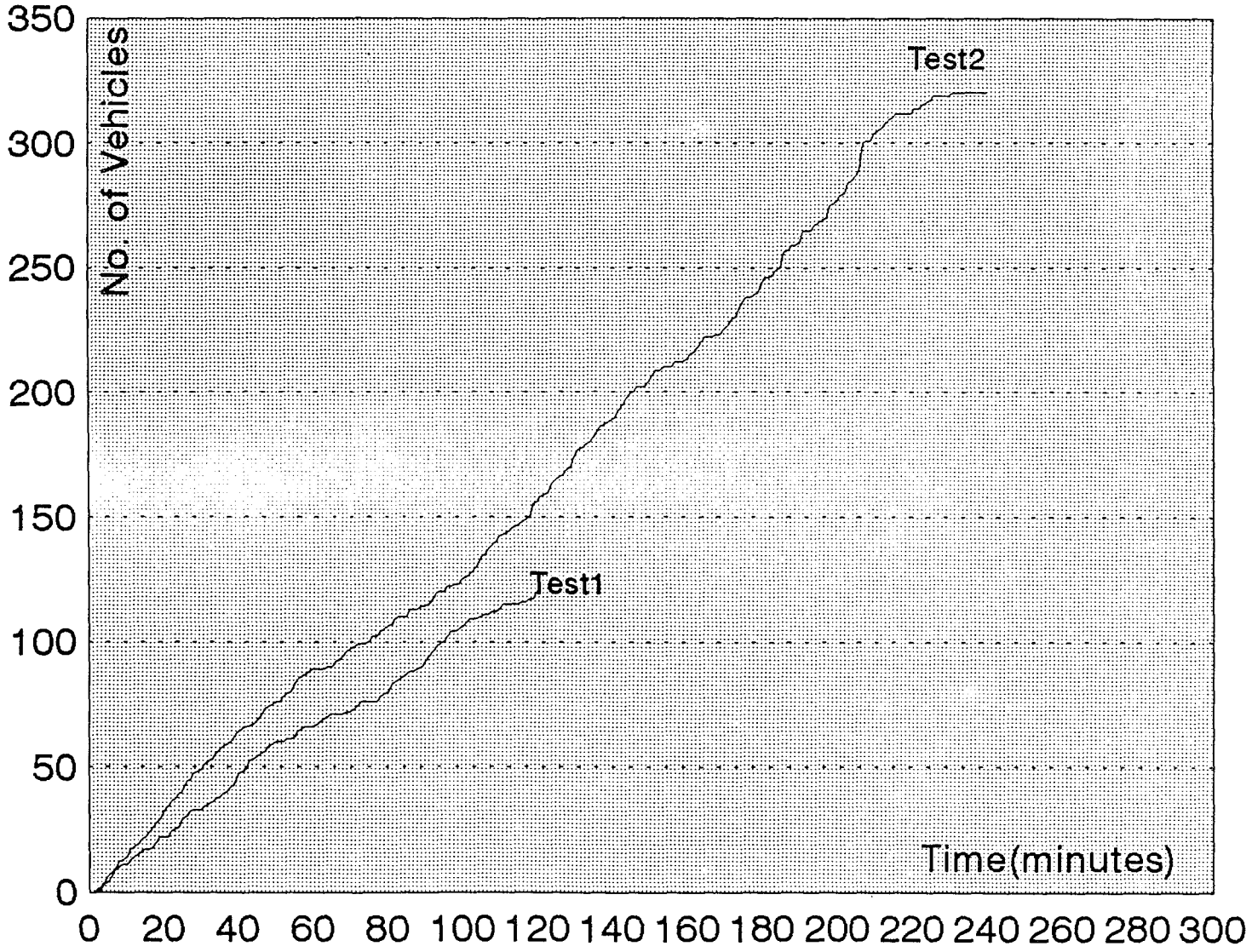

Figure.37Syracuse Computer Display Field's Tests

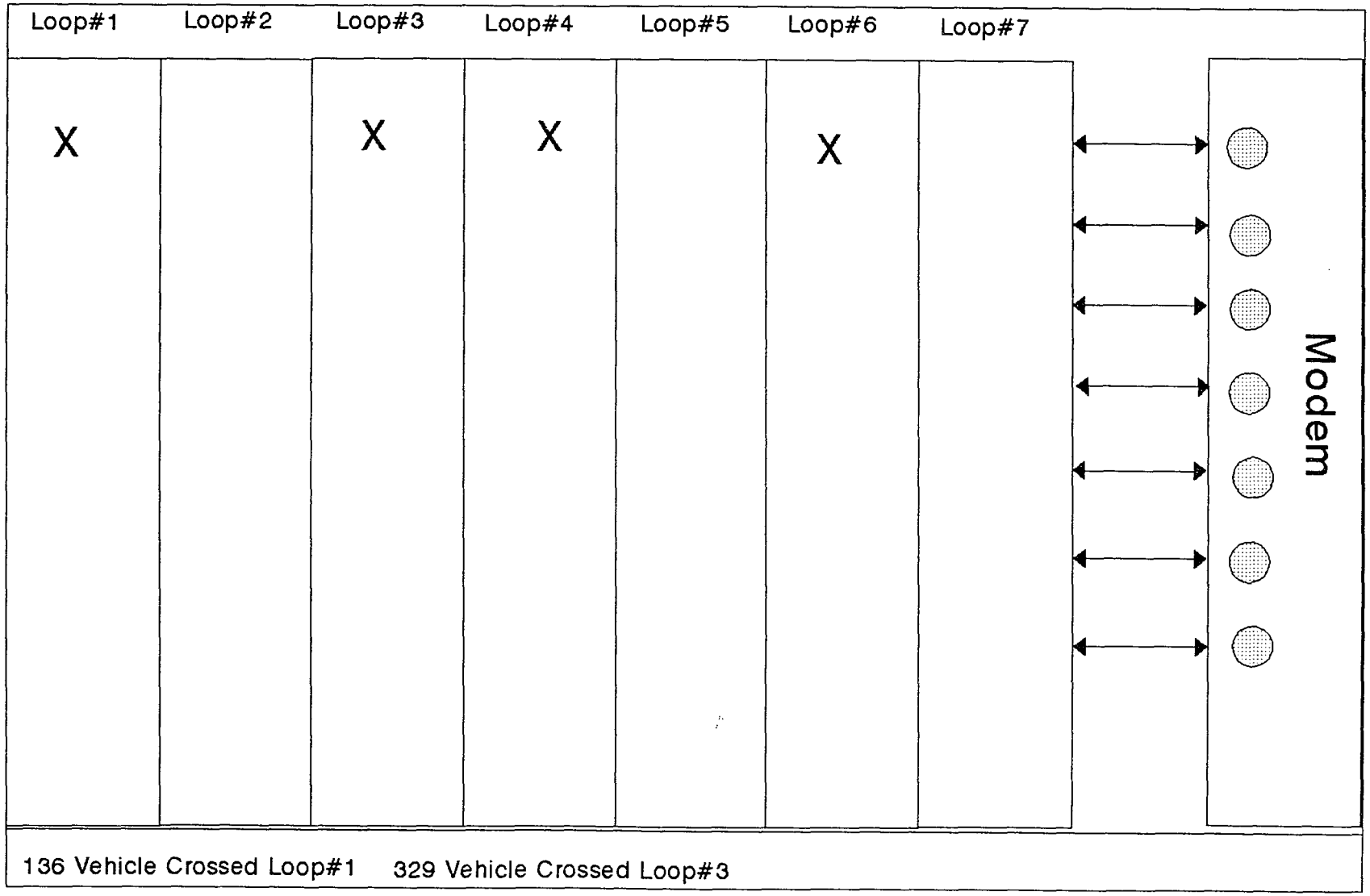

Figue.38 Loop Detector Recording Control Screen

BIBLIOGRAPHY :

[1]. "Traffic Detector-Technical Appendix", U.S. dep. Transportation, Fderal Highway Administration Implementation package, FHWA-IP-85-31, DC, April 1985.

[2]. "Traffic Detector Hand Book" U.S. Dep. of Transportation, Federal Highway Administration Implementation package, FHWA-IP-85-1, DC, April 1985.

[3]. Rafael M. Inigo, "Application of Machine Vision to Traffic Monitoring and Control" IEEE Transaction on Vehicular Technology, vol.38, No.3, pp. 112-122, August 1989.

[4]. Roland K. Jurgen, "Smarts Cars and Highways Go Global", IEEE Spectrum, pp. 26-36, May 1991.

[5]. R. Kent Gilbert and Quentin Holmes," Dynamic Traffic Information from Remote Video Monitor", Vehicle Navigation & Information Systems Conference Proceedings, pp. 213-231, October 1991.

[6]. Panos G. Michalopoulos, "Vehicle Detection Video Through Image Processing: The Autoscope System",IEEE Transactions on Vehicular Technology, vol.40, No.1, pp. 21-29, Feb.1991.

[7]. Robert J. Mayahan, Richard A. Bishel,"A Tow Frequency Radar for Vehicle Automatic Lateral Control", IEEE Transaction on Vehicular Technology, vol.vt-31,No.1, pp.85-93 Feb.1982.

[8]. Kiyo Tomiyasu, "Conceptual Performance of Bistatic Doppler Radar for Vehicle Speed Determination", IEEE Transactions on Vehicular Technology, vol.VT-30, No.3, pp. 130-134, August 1981.

[9]. T. Marakawa and T. Namewaka, "An Accurate System of FM-CW Radar for Approach Using Phase Detection", Electron. Communication , Japan, Vol 58-B,No.2, pp. 121-129, 1975.

[10].A. M. Nilson and G. F. Ross, "A New Radar Concept for Short Range Application," Research Paper, Sensor System

Department, Sperry Research Center, Sunbury, MA, Feb.1975.

[11].Jorge Bohmann, Heinrich Mayer, "A signal Processor for a Noncontact Speed/ Measurement System", IEEE Transaction on Vehicular Technology, vol. vt-33, No.1, pp.14-22, Feb. 1984.

[12].P.David Fisher, " Shortcomings of Radar Speed Measurement", IEEE Spectrum, pp. 28-31, December 1980.

[13].P. David Fisher, " Improve on Police Radar ", IEEE Spectrum, pp. 9-16, July 1992.

[14].David A. Hensher,"Electronic Toll Collection", Transportation Research, Section A, vol. 25A, No.1, pp. 15-21, 1991.

[15].Tarik Hussain, Tarek Saadawi & Samir Ahmed,"Overhead Infrared Vehicle Sensor For Traffic Control", ITE International Journal in transportation, pp. 38-45, September 1993.

[16].Tarik Hussain, Tarek Saadawi & Samir Ahmed,"Low Maintenance Overhead Vehicle Detector For Traffic Control", VINS91 Conference, Vol. p/253, pp. 455-463, 1991, sponsored by IEEE & SAE.

[17].PMI Data Book, CA, 1988.

[18].Texas Instruments TMS320 User's Guide, Texas, 1983.

[19].Keithely Metrabyte/ASYST/DAC, Data Acquisition and Control Manual, vol.23, NJ, 1990.

[20].Robert E. Tannin,"Fiberoptic Infrared and Laser Space Edge", Tab Book Inc., PA, 1987.

[21].Hamamatsu Photodiode's Catalog, NJ, 1991

[22].RCA Corporation, "Electro-Optics Handbook", LanCaster, PA, 1974.

[23].Walter Koechner, "Optical Ranging System Employing High Power Injection Laser Diode", IEEE Transaction on Aerospace and Electronic Systems, Vol. AES-4, No.1, pp. 81-91, Jan.1968.

[24].R.Salathe, W. Bolleter and H. Gilgen, " Long Range

Injection Laser Radar", Applied Optics, Vol.16, No.10, pp. 2621-2623, October 1977.

[25].Robert L. Anderson, "Loop Vehicle Detectors", IEEE Transaction on Vehicular Technology, pp.23-29, Dec. 1970.

[26].William Lynn, "Wright Laboratory Manual", FL, 1993.

[27].Merrill I. Skolnik, "Radar Handbook", 2nd. Edition, McGraw Hill, MI, 1989.

[28].G. Mamon, D.G. Youmans, Z.G. Sztankay and C.E. Mongan,"Pulsed GaAs Laser Terrain Profile", Applied Optics, Vol.17, pp. 868-875, March 1978.

[29].Tarik Hussain, Tarek Saadawi & Samir Ahmed,"Computerized Infrared Sensor To Detect Presence and Absence of Vehicles", Accepted for publication at the fifth international conference on Microelectronics, December 1993, Saudi Arabia.

[30].Tarik Hussain, Tarek Saadawi & Samir Ahmed,"Infrared Pyroelectric Sensor For Detection of Vehicular Traffic Using Digital Signal Processing Techniques", Submitted to IEEE Transaction on Vehicular Technology for reviewing.

[31].ELTEC Instruments, Inc., Manual, FL, 1991

Table 1: Photodiodes Types

Type	Connection	Features	Photodiode Types
Planar Diffusion Type	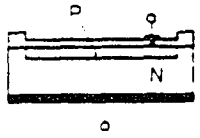	Small Dark Current	Silicon Photodiodes GaAsP Photodiodes
Low Cj Planar Diffusion Type	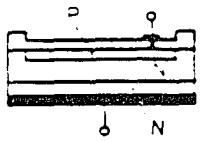	Small Dark Current, Fast Response, High UV Sensitivity , Suppressed IR Sensitivity	Silicon Photodiodes
PIN-Type	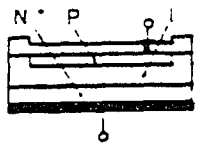	Ultra-Fast Response	PIN Silicon Photodiodes
PNN- Type	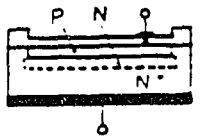	Small dark Current, Fast Response, High UV Sensitivity , Suppressed IR Sensitivity	Silicon Photodiodes
Schottky Type	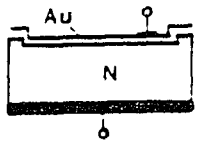	High Ultraviolet Sensitivity	GaAsP, Gap Photodiodes
Avalanche Type	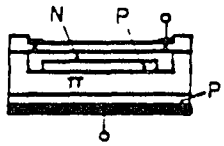	Internal Multiplying Mechanism Ultra-Fast Response	Silicon Avalanche Photodiodes

Table.2

Silicon Photodiodes (UV to IR, For Precision Photometry)

Type No. Ⓐ	Outline Ⓑ	Package (mm)	Photosensitive Surface: Size (mm)	Photosensitive Surface: Effective Area (mm²)	Spectral Response: Range (nm)	Spectral Response: Peak Wavelength (nm)	Characteristics (25°C): Radiant Sensitivity (A/W): Peak Wavelength Typ.	200nm: Min.	200nm: Typ.	633nm He-Ne Laser Typ.	930nm GaAs LED Typ.	Short Circuit Current I_{SC} 100: Min. (μA)
S1336 Series (Metal Case)												
S1336-18BQ	❶	TO-18	1.1×1.1	1.2	190~1000	960	0.5	0.08	0.1	0.33	0.5	1
-18BK					320~1000			–	–			
-5BQ	❼	TO-5	2.4×2.4	5.7	190~1000			0.08	0.1			4
-5BK					320~1000			–	–			
-44BQ			3.6×3.6	13	190~1000			0.08	0.1			8
-44BK					320~1000			–	–			
-8BQ	❿	TO-8	5.8×5.8	33	190~1000			0.08	0.1			22
-8BK					320~1000			–	–			
S1337 Series (Ceramic Case)												
S1337-16BQ	⓮	2.7×15	1.1×5.9	5.9	190~1000	960	0.5	0.08	0.1	0.33	0.5	4
-16BR	⓯				320~1000		0.62	–	–	0.4	0.6	4.4
-33BQ	⓰	6×7.6	2.4×2.4	5.7	190~1000		0.5	0.08	0.1	0.33	0.5	4
-33BR	⓱				320~1000		0.62	–	–	0.4	0.6	4.4
-66BQ	⓲	8.9×10.1	5.8×5.8	33	190~1000		0.5	0.08	0.1	0.33	0.5	20
-66BR	⓳				320~1000		0.62	–	–	0.4	0.6	22
-1010BQ	⓴	15×16.5	10×10	100	190~1000		0.5	0.08	0.1	0.33	0.5	65
-1010BR	㉑				320~1000		0.62	–	–	0.4	0.6	70